

TDK dolgozat

Polcz Péter

PÁZMÁNY PÉTER KATOLIKUS EGYETEM
INFORMÁCIÓS TECHNOLÓGIAI ÉS BIONIKAI KAR

**Továbbfejlesztett módszer bizonytalan
nemlineáris rendszerek stabilitási tartományának
becslésére**

(An improved method for estimating the domain of attraction of
uncertain nonlinear systems)

Szerző:
POLCZ Péter
6. évfolyam (MSc)

Témavezető:
Dr. SZEDERKÉNYI Gábor
egyetemi tanár

Abstract

An optimization based method is proposed in this report for the computation of Lyapunov functions and regions of attractions for uncertain nonlinear systems containing polynomial and rational terms. The Lyapunov function is given in a special quadratic form, and the negativity of its derivative is ensured by the application of appropriate LMI conditions. The starting point of the method is an approach taken from the literature, in which the conservatism of the solution is reduced by utilizing Finsler's lemma. The improvements and new contributions can be summarized as follows: 1) The transformation of the model to the form required for optimization is done automatically. At the same time, the number of monomials and rational terms in the computational problem is kept as low as possible using linear fractional transformation (LFT) and further automatic model simplification steps. This technique results in the dimension reduction of the problem compared to other solutions known from the literature. 2) An algorithm was given for the generation of suitable annihilators, which appear in Finsler's lemma. 3) An improved method was proposed for determining the largest possible invariant set for the dynamics using the computed Lyapunov function. 4) In comparison with the technique taken from the literature, a generalized and simplified formula was given for the LMI condition, which ensures negativity of the time derivative of the Lyapunov function. The operation of the method is illustrated on a seven examples taken from the literature.

Based on this work, an international journal paper [9] and a research report [10] was published.

Contents

1	Introduction	2
1.1	Notations, abbreviations	4
2	Basic notions, known results	5
2.1	Linear matrix inequalities	5
2.2	System class, Lyapunov functions, domain of attraction	7
2.3	Sufficient LMI conditions for stability using Finsler’s lemma and the notion of annihilators	8
2.4	Dynamical system representation	10
2.5	Linear fractional transformations	11
3	Estimating the domain of attraction	12
3.1	Handling polynomial terms	13
3.2	Eliminating repetitive terms	13
3.3	Annihilator generation	14
3.4	Finding an appropriate Lyapunov function	17
3.5	Finding the maximal level set for a given polytope	20
3.6	Finding the most appropriate outer polytope	23
3.7	Dimensions of the optimization problem	24
4	Illustrative examples and results	25
4.1	Van der Pol dynamics	26
4.2	Uncertain Van der Pol dynamics	28
4.3	Mass-action kinetic systems	32
4.3.1	Time inverted Sel’kov model	32
4.3.2	Minimal MAK system with an unbounded DOA	34
4.4	Third order rational system	36
4.5	Stability of a controlled inverted pendulum	38
4.6	A continuous fermentation process	41
4.6.1	Open-loop system (OLS)	44
4.6.2	Effect of linear substrate feedback	45
5	Conclusions	47

1. Introduction

Approximating the domain of attraction (DOA) is often a fundamental task in model analysis and controller design/evaluation. The stability properties of dynamical systems are most often studied using Lyapunov functions, accordingly, the computational construction of Lyapunov functions [11] has been addressed extensively in the literature.

It is well-known that the DOA of an asymptotically stable equilibrium point of a dynamical system $\dot{x} = f(x)$, $x \in \mathbb{R}^n$ can be precisely determined in theory by solving Zubov's first order nonlinear partial differential equation [12]. There exist many generalizations of Zubov's method, for example, the paper [13] is dedicated to determine the *robust* domain of attraction of an uncertain system $\dot{x}(t) = f(x(t), \delta(t))$, where $\delta : \mathbb{R} \mapsto \mathcal{D}$ is a bounded perturbation and \mathcal{D} is a compact subset of \mathbb{R}^d , furthermore, it is assumed that $f(0, \delta) = 0$ for all δ in \mathcal{D} . In case of uncertain dynamical systems, the DOA is called *robust*, furthermore, it is the set of points from which the system converges to the equilibrium point regardless of the actual values of the uncertain parameters. The main disadvantage of this method is that the solvability of Zubov's partial differential equation cannot be foreseen.

Another fundamental result in this field is the existence of the so-called maximal Lyapunov functions for a wide class of nonlinear systems and the corresponding partial differential equation which characterizes them [14]. In comparison with Zubov's equation, an iterative procedure is given for approximating the maximal *rational* Lyapunov function. An algorithm for generating Lyapunov functions for a special class of nonlinear systems based on the construction of polytopes is given in [15]. In [16], a linear programming based method is given for the construction of Lyapunov functions for general planar nonlinear systems. In [17], maximal Lyapunov functions were defined and computed for hybrid (piecewise nonlinear) systems.

At the same time, the use of linear matrix inequalities (LMI) and semidefinite programming (SDP) techniques for nonlinear systems has become very popular due to their advantageous properties and the availability of efficient numerical tools to solve LMI problems. These new techniques provide a powerful framework for stability analysis, robust control and filtering problems. Ghaoui et.al. [18] used quadratic Lyapunov functions and linear fractional transformations (LFT) to represent a rational nonlinear

system and defined convex conditions for stability analysis and state feedback design. A method that applies sum of squares (SOS) programming to maximize the estimate of the region of attraction can be found in [11, 19]. Stability conditions in both references are converted into LMIs using SOS relaxations and the generalization of the S-procedure. Topcu et.al. [20] utilized a further branch-and-bound type refinement in the parameter space to reduce the solution’s conservatism.

A recent important result from this line of research is published in [1], where the authors use Finsler’s lemma and the notion of annihilators to compute rational Lyapunov functions for a wide class of locally asymptotically stable nonlinear systems. The newly introduced sufficient conditions for the stability are affine parameter dependent LMIs, because they are characterized by affine functions of the state x and the uncertain parameters represented by the column vector δ . Affine parameter dependent LMIs can be computationally handled by checking their feasibility at the corner points (vertices) of a polytope (convex region), on which the state and uncertain parameters are defined. These LMI conditions are obtained from the prescribed properties of a Lyapunov function having monomial and rational terms. In case of uncertain systems, the (possibly time-dependent) uncertain parameters will also appear in the Lyapunov function. A key point in this method is to find the largest possible polytope $\mathcal{X} \subset \mathbb{R}^n$ (subset of the state space), on which the Lyapunov conditions are satisfied. After \mathcal{X} is computed, the domain of attraction is estimated by an invariant set, that is the maximal closed level set ε of the Lyapunov function being located completely inside of \mathcal{X} . In order to find a “good” polytope \mathcal{X} , the authors constructed an initial polytope $\mathcal{X}^{(0)}$, then through the iteration steps the area/volume of $\mathcal{X}^{(i)}$ is increased considering the shape of the obtained maximal invariant level set $\varepsilon^{(i)}$. The authors present further techniques to cope with non-convex regions (unions of polytopes). In [1], it is also shown that with some additional conservatism, the application of predefined polytopes can be avoided by modifying the LMIs with the S-Procedure [21].

This work is based on the results of [1], and introduces an improved method to generate sufficient LMI conditions for local asymptotic stability of polynomial and rational nonlinear systems. In comparison with [1], the LMI conditions are generated automatically using the linear fractional transformation (LFT). In order to decrease the dimension of the optimization problem, further algebraic model transformation steps are proceeded. In Section 3.3, the properties and effects of an annihilator are discussed and an algorithm is presented to generate appropriate annihilators. Sections 3.4 and 3.5 present the whole mathematical procedure and their formulas borrowed from [1] in a simplified, generalized framework. In the last chapter, computational results are presented on illustrative planar and third order models taken from the literature, and additionally static and dynamic feedback control laws are applied

This report does not address the handling of non-convex regions or union of poly-

topes. The aim is to develop an autonomous mathematical apparatus for dealing with symbolically complex and/or higher order dynamical models but using relatively simple \mathcal{X} polytopes, on which Lyapunov conditions can be easily tested. Furthermore, assuming rectangular polytopes¹, the iterative procedure to evaluate (enlarge) the polytope \mathcal{X} can be easily automated.

1.1 Notations, abbreviations

In this report, I will use the following notations and abbreviations:

1. linear matrix inequality (LMI)
2. semidefinite programming/problem (SDP)
3. domain of attraction (DOA)
4. an optimization problem aims to find the optimal value of an objective function subject to a variable called *decision variable* (d.v.)
5. linear fractional transformation/representation (LFT/LFR)
6. open-loop system (OLS), closed-loop system (CLS)
7. $i = \overline{1, n}$ means $i \in \{1, \dots, n\}$
8. $\text{Co}(\mathcal{X})$ denotes the convex expansion of a bounded polytope \mathcal{X} , more specifically, $\text{Co}(\{v_i \mid i = \overline{1, n}\})$ is the convex hull of the set of vertices $\{v_i \mid i = \overline{1, n}\}$.
9. $\vartheta(\mathcal{X})$ denotes the set of all vertices (corner points) of the convex polytope \mathcal{X} (i.e. $\text{Co}(\vartheta(\mathcal{X})) = \mathcal{X}$).
10. $\nabla V(x)$ is the gradient of the scalar function $V(x)$.
11. $0_{n \times m}$ and I_n denote the $n \times m$ zero matrix and $n \times n$ unit matrix, respectively.
12. Kronecker product: $A \otimes B = \begin{bmatrix} a_{11}B & \cdots & a_{1m}B \\ \vdots & \ddots & \vdots \\ a_{n1}B & \cdots & a_{nm}B \end{bmatrix} = \text{kron}(A, B)$
13. $[a_i]_{\text{col}}^{i=\overline{1, n}} = [a_1 \ \cdots \ a_n]^T$
14. $[a_i]_{\text{row}}^{i=\overline{1, n}} = [a_1 \ \cdots \ a_n]$
15. $\text{row}_i(A)$ denotes the i th row of matrix A
16. $\text{col}_i(A)$ denotes the i th column of matrix A

¹hyperrectangle, Cartesian product of intervals

2. Basic notions, known results

In this section, I present the basic notions, further notations and known results on which my computational results are based.

2.1 Linear matrix inequalities (LMI)

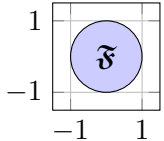
Linear matrix inequalities are convex conditions of the following form:

$$F(x) = F_0 + \underbrace{\sum_{i=1}^n x_i F_i}_{\text{canonical form of LMIs}} > 0 \quad (2.1)$$

This form can also be considered as the canonical form of the LMIs, in which the $F_{i=0,\overline{n}} \in \mathbb{R}^{m \times m}$ are fixed constant symmetric matrices and $x = (x_i)_{i=1,\overline{n}} \in \mathbb{R}^n$ are free variables, so called *decision variables* of the LMI. The inequality operator “>” means that $F(x)$ is a positive definite matrix, namely $\eta^T F(x) \eta > 0$ for all $\eta \in \mathbb{R}^m \setminus \{0\}$.

An LMI is *feasible* if there exists $x \in \mathbb{R}^n$, such that $F(x) > 0$, correspondingly, the set $\mathfrak{F} = \{x \mid F(x) > 0\}$ is called the *feasibility set* of the inequality (2.1). An LMI is a convex constraint in the sense that its feasibility set is a convex set, more specifically, if $x, y \in \mathfrak{F}$ than $\lambda x + (1 - \lambda)y \in \mathfrak{F}$ for all $\lambda \in [0, 1]$.

Example 1. Consider the unit disc as the feasibility set \mathfrak{F} , and its corresponding quadratic condition:



$$: x_1^2 + x_2^2 \leq 1 \Leftrightarrow 1 - x^T I_2 x \geq 0$$

By using the Schur complement lemma (for more details, see [22]), this inequality can be converted into an equivalent LMI condition:

$$\begin{bmatrix} I_2 & x \\ x^T & 1 \end{bmatrix} \geq 0 \Leftrightarrow \begin{bmatrix} 1 & 0 & 0 \\ 0 & 1 & 0 \\ 0 & 0 & 1 \end{bmatrix} + x_1 \begin{bmatrix} 0 & 0 & 1 \\ 0 & 0 & 0 \\ 1 & 0 & 0 \end{bmatrix} + x_2 \begin{bmatrix} 0 & 0 & 0 \\ 0 & 0 & 1 \\ 0 & 1 & 0 \end{bmatrix} \geq 0 \quad (2.2)$$

This example demonstrates a simple LMI condition and its feasibility set (unit disc).

The canonical form of a semidefinite problem (SDP) can be formulated as follows:

$$\min c^T x \quad \text{s.t.} \quad F_0 + \sum_{i=1}^n x_i F_i > 0 \quad (2.3)$$

In this optimization task, $c^T x$ is the objective function to be minimized, additionally, the LMI defines a convex set, containing the possible values of vector x . The parameter $c \in \mathbb{R}^n$ appearing in the objective function is a constant predefined column vector.

In this report, the LMIs will appear in another common form:

$$X + YB + B^T Y^T \geq 0 \quad (2.4)$$

where $B \in \mathbb{R}^{q \times m}$ is a constant matrix, $X \in \mathbb{R}^{m \times m}$ and $Y \in \mathbb{R}^{m \times q}$ are variables (with X being symmetric) comprising $\frac{m(m+1)}{2}$ and qm pieces of free parameters in the computations. This LMI condition can be easily converted into its canonical form as presented in [22], as equations (16,17,18).

2.2 System class, Lyapunov functions, domain of attraction

I consider nonlinear systems of the form

$$\dot{x}(t) = f(x(t), \delta(t)) \quad x(t) \in \mathbb{R}^n, \quad x_0 \in \mathcal{X}, \quad \delta(t) \in \mathcal{D}, \quad \dot{\delta}(t) \in \check{\mathcal{D}} \quad (2.5)$$

- $\mathcal{X} \subset \mathbb{R}^n$ and $\mathcal{D}, \check{\mathcal{D}} \subset \mathbb{R}^d$ bounded polytopes
- $x : \mathbb{R} \mapsto \mathcal{X}$ state vector function, $x_0 = x(0)$ is the initial condition
- $\delta : \mathbb{R} \mapsto \mathcal{D}$ smooth, bounded vector function with bounded derivative representing the uncertain parameters
- $f : \mathcal{X} \times \mathcal{D} \mapsto \mathbb{R}^n$ well defined smooth rational mapping, $f(0, \delta) = 0, \forall \delta \in \mathcal{D}$, i.e., $x^* = 0 \in \mathbb{R}^n$ is a locally asymptotically stable equilibrium point of (2.5) for all $\delta \in \mathcal{D}$

In the future, the time arguments of x and δ will be suppressed as it is commonly done in the literature. The set of all initial conditions, from which the solutions converge to x^* is called the *domain of attraction* (DOA).

I am looking for an appropriate rational Lyapunov function $V(x, \delta)$ which satisfies the following conditions:

$$\begin{aligned} v_l(x) \leq V(x, \delta) \leq v_u(x) \quad \forall (x, \delta) \in \mathcal{X} \times \mathcal{D} \\ \dot{V}(x, \delta, \dot{\delta}) \leq -v_d(x) \quad \forall (x, \delta, \dot{\delta}) \in \mathcal{X} \times \mathcal{D} \times \check{\mathcal{D}} \end{aligned} \quad (2.6)$$

where v_l , v_u and v_d are continuous positive functions on \mathcal{X} . Clearly, if the inequalities in (2.6) are fulfilled, then any closed level set of V contained (entirely) by \mathcal{X} bounds an invariant region of the state space that is part of the DOA.

The measure of *conservatism* is a property, which describes an invariant region. Let us consider two domains ε and γ bounded by two different level sets. I call ε less *conservative* than γ if ε is a better estimate of the actual DOA in the sense that the area/volume of ε is larger than that of γ . In a similar fashion, an inequality condition (A) is considered more conservative than condition (B) if (A) implies (B), alternatively, if the feasibility set of (A) is a subset of the feasibility set of (B): $\mathfrak{F}_A \subset \mathfrak{F}_B$.

Roughly speaking, the main objective is to find a Lyapunov function $V(x)$ having a level set, which bounds the achievable least conservative invariant region. In fact, introducing higher degree monomials into $V(x)$ generally results in better estimates, although a small increment in the number of monomials generates a huge increase in the dimension of the problem. Therefore, the rapidly growing computational burden must be taken into consideration through considering the possibilities of dimension reduction.

2.3 Sufficient LMI conditions for stability using Finsler's lemma and the notion of annihilators

In the case of a linear time invariant (LTI) dynamical system $\dot{x} = Ax$, with a quadratic Lyapunov function candidate $V(x) = x^T Px$, the necessary and sufficient Lyapunov conditions (2.6) for the system's global stability can be easily converted into their *equivalent* LMI form: $P > 0$ (P is positive definite), and $PA + A^T P < 0$.

On the contrary, when having an uncertain linear system $\dot{x} = \mathcal{A}(\delta)x$ with an *affine* state transition matrix function $\mathcal{A}(\delta)$, the Lyapunov inequality regarding negativity of the derivative of $V(x)$ will dependent on the parameter δ . According to Proposition 2.3.2, if we can specify a bounded polytope \mathcal{D} in which the uncertain parameter δ remains, then it is enough to test the inequality in the corner points of \mathcal{D} : $P\mathcal{A}(\delta) + \mathcal{A}(\delta)^T P < 0$, for all $\delta \in \vartheta(\mathcal{D})$. This system of LMIs is still *equivalent* to the second inequality of (2.6).

Formulating equivalent LMI conditions is not straightforward when having a nonlinear system of the form $\dot{x} = \mathcal{A}(x)x$, or in case of a non-quadratic polynomial (or rational) Lyapunov function.

In [1], the authors are looking for a Lyapunov function in the form

$$V(x, \delta) = \pi_b^T(x, \delta) P \pi_b(x, \delta) \quad (2.7)$$

where $P \in \mathbb{R}^{m \times m}$ is a constant symmetric matrix, $\pi : \mathbb{R}^n \times \mathcal{D} \mapsto \mathbb{R}^p$ is a smooth mapping, in which each element is a smooth rational function in x and δ , but $\pi(x, \delta)$ does not contain the linear terms $x_{i=\overline{1, n}}$. Finally, the mapping $\pi_b : \mathbb{R}^n \times \mathcal{D} \mapsto \mathbb{R}^{m=n+p}$ is defined as $\pi_b(x, \delta) = [x, \pi]_{\text{col}}$. In the future, the arguments of π and π_b will be omitted.

Using Finsler's lemma, one can formulate sufficient LMI conditions, which imply the Lyapunov conditions.

Lemma 2.3.1 (Finsler's lemma)

Let $\Omega \subseteq \mathbb{R}^s$ be a predefined bounded polytope, $P : \Omega \mapsto \mathbb{R}^{m \times m}$, $N : \Omega \mapsto \mathbb{R}^{q \times m}$ be given matrix functions, with $P(\omega)$ symmetric. Let $Q : \Omega \mapsto \mathbb{R}^{m \times (m-r)}$ be a matrix function having the basis vectors of the null space of $N(\omega)$ as its columns, i.e. $N(\omega)Q(\omega) = 0$, where r denotes the number of linearly independent rows of $N(\omega)$. Then, the following are equivalent:

- (i) $\forall \omega \in \Omega, \forall \pi_b : \Omega \mapsto \mathbb{R}^m \quad [N(\omega)\pi_b(\omega) = 0 \rightarrow \pi_b^T(\omega)P(\omega)\pi_b(\omega) > 0]$
- (ii) $\exists L : \Omega \mapsto \mathbb{R}^{m \times q} \quad [\forall \omega \in \Omega \quad [P(\omega) + L(\omega)N(\omega) + N^T(\omega)L^T(\omega) > 0]]$
- (iii) $\forall \omega \in \Omega \quad [Q^T(\omega)P(\omega)Q(\omega) > 0]$.

The lemma is also presented in [1], and an alternative form of it can be found in [23], its proof is presented in [24].

Remark. $N(\omega)$ is called an *annihilator* of $\pi_b(\omega)$ due to the equality $N(\omega)\pi_b(\omega) = 0$. An annihilator has an important role in the LMI condition by making it less conservative.

Assuming that $P(\omega)$ and $N(\omega)$ are affine functions and L is a constant matrix, one can obtain a special case of Finsler's lemma. In that case, the conditions (i) and (ii) are no longer equivalent, but (ii) still implies (i). Furthermore, (ii) will become a polytopic LMI (i.e. an affine parameter dependent LMI over a bounded polytopic region) of the following form

$$\exists L \in \mathbb{R}^{m \times q} \left[\forall \omega \in \Omega \left[P(\omega) + LN(\omega) + N^T(\omega)L^T > 0 \right] \right] \quad (2.8)$$

As stated previously, this polytopic LMI can be transformed into a parameter independent system of LMIs by using the following proposition presented in [4] as Proposition 5.4.

Proposition 2.3.2 *The LMI (2.8) is satisfied if and only if there exists a matrix $L \in \mathbb{R}^{m \times q}$ such that $P(\omega) + LN(\omega) + N^T(\omega)L^T > 0$ holds for every **corner point** (i.e. vertex) of Ω , i.e. $\forall \omega \in \vartheta(\Omega)$.*

Returning to the Lyapunov function (2.7), a sufficient condition can be formulated for its positivity if we can find an appropriate affine annihilator $N(x, \delta)$ in such a way that $N(x, \delta)\pi_b = 0$ for all $(x, \delta) \in \mathcal{X} \times \mathcal{D}$.

Example 2. In this example, I want to demonstrate how an annihilator can bring more freedom into an LMI condition by taking into account the algebraic relationship between the coordinates of π_b . First of all, examine the following possible values of π_b and that of its annihilator $N(x)$:

$$x = \begin{bmatrix} x_1 \\ x_2 \end{bmatrix}, \quad \pi = \begin{bmatrix} x_1^2 \\ x_1 x_1 x_2 \end{bmatrix}, \quad \pi_b = \begin{bmatrix} x_1 \\ x_2 \\ x_1^2 \\ x_1 x_2 \end{bmatrix}, \quad N(x) = \begin{bmatrix} x_2 & -x_1 & 0 & 0 \\ x_1 & 0 & -1 & 0 \\ x_2 & 0 & 0 & -1 \end{bmatrix} \quad (2.9)$$

The domain of interest is the unit square, namely: $\mathcal{X} = [-1, 1] \times [-1, 1]$. Indeed, $N(x)\pi_b = 0$ for every x in \mathcal{X} , furthermore, it is obvious that

$$P + LN(x) + N^T(x)L^T > 0 \quad (2.10)$$

is a less conservative sufficient condition for $\pi_b^T P \pi_b > 0$, than $P > 0$. In order to experience the effect of the annihilator, let us consider the following possible numerical

values of P and L :

$$P = \begin{bmatrix} 1.8 & 0 & 0 & 0 \\ 0 & 1.2 & 0 & 0 \\ 0 & 0 & -0.5 & 0 \\ 0 & 0 & 0 & 1.2 \end{bmatrix}, \quad L = \begin{bmatrix} 0 & 0 & 0 \\ 0 & 0 & 0 \\ 0 & -0.79 & 0 \\ 0.02 & 0 & -0.048 \end{bmatrix}$$

P is definitely not a positive definite matrix because it has a negative eigenvalue (-0.5), however, the condition (2.10) is satisfied for each corner point of the polytope \mathcal{X} : $\forall x \in \vartheta(\mathcal{X}) = \{(1, 1), (-1, 1), (-1, -1), (1, -1)\}$

In Section 3.3, I will present the issue of the annihilator generation in detail.

2.4 Dynamical system representation

Using the variables from equations (2.5,2.7), I present a similar differential-algebraic representation of nonlinear models that was introduced in [1]:

$$\begin{aligned} \dot{x} &= f(x, \delta) = Ax + B\pi \quad x_0 \in \mathcal{X} \\ 0 &= \mathcal{N}_{\pi_b}(x, \delta)\pi_b \quad \delta \in \mathcal{D}, \dot{\delta} \in \check{\mathcal{D}} \end{aligned} \tag{2.11}$$

In comparison with (2.7), $\pi = \pi(x, \delta) \in \mathbb{R}^p$ is a column vector function containing *only* monomials in (x, δ) , except the x_i linear elements, or rational terms with monomial numerators.

This form separates the linear part of the system (x) from its nonlinear part (π). In case of polynomial systems, the authors of [1] propose that π contains all monomials of degree less than or equal to the maximal degree term in the system equation. This clearly causes a combinatorial explosion as the number of variables and their degrees increase. Therefore, I propose the application of LFT to decrease the number of elements of column vector π , expecting that the solutions conservatism will not increase significantly. In Section 3.7., I made a detailed study on the dimensions of the optimization problem, and how they are affected by the number of elements in π .

2.5 Linear fractional transformation (LFT)

The LFT is discussed in detail in book [25, Chapter 10.]. This transformation plays an important role in modeling uncertain rational systems, and it is often used in literature, as presented in [18]. Using the LFT the linear and nonlinear part of any rational nonlinear uncertain system of the form $\dot{x} = \mathcal{A}(x, \delta)x$ can be separated in the following manner:

$$\begin{array}{c} \begin{array}{|c|c|} \hline M_{11} & M_{12} \\ \hline M_{21} & M_{22} \\ \hline \end{array} \begin{array}{l} \leftarrow x \\ \leftarrow w \end{array} \\ \begin{array}{c} \dot{x} \\ z \end{array} \begin{array}{l} \leftarrow \\ \leftarrow \end{array} \\ \Delta(x, \delta) \end{array} \quad \begin{array}{l} \begin{bmatrix} \dot{x} \\ z \end{bmatrix} = \begin{pmatrix} M_{11} & M_{12} \\ M_{21} & M_{22} \end{pmatrix} \cdot \begin{bmatrix} x \\ w \end{bmatrix} \leftrightarrow \begin{array}{l} \dot{x} = M_{11}x + M_{12}w \\ z = M_{21}x + M_{22}w \end{array} \end{array} \quad (2.12)$$

$$w = \Delta(x, \delta) z \quad (2.13)$$

where M_{ij} are constant matrices and $\Delta(x, \delta)$ is a diagonal matrix function of the state variables and uncertain parameters.

Equation (2.12) can be considered as a linear time invariant (LTI) differential-algebraic equation with a nonlinear input defined by the nonlinear uncertain function (2.13). By eliminating z and w from (2.12) and (2.13) and by using an auxiliary step, one can get the following:

$$\mathcal{A}(x, \delta)x = \underbrace{M_{11}x}_{\text{linear part}} + \underbrace{M_{12}(I_p - \Delta(x, \delta)M_{22})^{-1}\Delta(x, \delta)M_{21}x}_{\text{nonlinear part}}, \quad (2.14)$$

According to Definition 10.2 of [25], an LFT is said to be well defined (or well-posed) if $(I_p - \Delta(x, \delta)M_{22})$ is invertible for all $(x, \delta) \in \mathcal{X} \times \mathcal{D}$.

The auxiliary step during the evaluation of the right hand side of equation (2.14) constitutes the following identity (the arguments in Δ will be suppressed):

$$\Delta(I_p - M_{11}\Delta)^{-1}M_{21} = (I_p - \Delta M_{11})^{-1}\Delta M_{21} \quad (2.15)$$

This identity can be easily seen, if I_p is substituted by $\Delta^{-1}\Delta$, than the left hand side of (2.15) will be:

$$\Delta((\Delta^{-1} - M_{11})\Delta)^{-1}M_{21} = (\Delta^{-1} - M_{11})^{-1}M_{21} = (\Delta^{-1} - M_{11})^{-1}I_p M_{21} \quad (2.16)$$

The same idea is applied on the newly introduced I_p :

$$(\Delta^{-1} - M_{11})^{-1}\Delta^{-1}\Delta M_{21} = (\Delta(\Delta^{-1} - M_{11}))^{-1}\Delta M_{21} = (I_p - \Delta M_{11})^{-1}\Delta M_{21} \quad (2.17)$$

Note that the first equation of (2.12) resembles the first equation of (2.11). In the next section, we will see that by choosing $\pi = w$, $A = M_{11}$, $B = M_{12}$, we will get the same representation as in (2.11). Furthermore, composing an annihilator matrix for $\pi_b = [x, \pi]_{\text{col}}$ will also be a quite straightforward operation.

3. Estimating the domain of attraction

Since the linear fractional representation (LFR) in equations (2.12, 2.13) is a special case of (2.11), it can be easily transformed into the general form by introducing the following notations:

$$\begin{aligned}
 A = M_{11} \quad G(x, \delta) = -\Delta(x, \delta)M_{21} & \in \mathbb{R}^{p \times n} \\
 B^{(0)} = M_{12} \quad F(x, \delta) = I_p - \Delta(x, \delta)M_{22} & \in \mathbb{R}^{p \times p} \\
 \pi^{(0)} = w = -F^{-1}(x, \delta)G(x, \delta)x \in \mathbb{R}^p & \\
 \mathcal{N}_{\pi_b}^{(0)}(x, \delta) = [G(x, \delta) \quad F(x, \delta)] & \text{ is an annihilator of } \pi_b = [x, \pi]_{\text{col}}
 \end{aligned} \tag{3.1}$$

We assume that the LFT is well-posed, i.e. the matrix function F is invertible for all $(x, \delta) \in \mathcal{X} \times \mathcal{D}$. The superscripts (i) in case of $B^{(0)}$, $\mathcal{N}_{\pi_b}^{(0)}(x, \delta)$ and $\pi^{(0)}$ suggest that these variables will be modified during some further algebraic steps. In case of π_b , the superscript (i) will be suppressed, even though, π_b will also be modified as well through the modifications applied on π .

By using the LFT, the following issues emerge that need to be handled:

1. The generated $\pi^{(0)}$ may contain polynomial functions or rational terms with polynomial numerators.
2. The variables $\pi^{(0)}$ may contain redundant (linearly dependent or repetitive) elements.
3. In general, the newly generated annihilator $\mathcal{N}_{\pi_b}^{(0)}(x, \delta)$ can be supplemented by further annihilator rows, which will introduce further independent decision variables into the optimization problem, consequently, the LMIs will become less conservative.

In the next three sections, I propose a possible resolution for each issue.

3.1 Handling polynomial terms

Considering the properties of the LFR, I can assume that $\pi^{(0)}$ contains only rational terms. In this case, the task is to split up the elements with a polynomial numerator, but then, the size of $\pi^{(0)}$ will increase significantly. In order to ensure that the model equations (2.11) hold, it is necessary to modify the related columns of the left multipliers of $\pi^{(0)}$ (i.e. $B^{(0)}$ and $\mathcal{N}_{\pi_b}^{(0)}(x, \delta)$) appropriately. The following equation demonstrates this procedure:

$$\underbrace{\begin{bmatrix} f(x, \delta) \end{bmatrix}}_{\text{left multiplier}} \underbrace{\begin{bmatrix} \frac{\alpha p(x, \delta) + \beta q(x, \delta)}{r(x, \delta)} \end{bmatrix}}_{\pi^{(0)}} = \underbrace{\begin{bmatrix} \alpha f(x, \delta) & \beta f(x, \delta) \end{bmatrix}}_{\text{modified left multipliers}} \underbrace{\begin{bmatrix} \frac{p(x, \delta)}{r(x, \delta)} \\ \frac{q(x, \delta)}{r(x, \delta)} \end{bmatrix}}_{\pi^{(1)}}, \quad (3.2)$$

where $p(x, \delta)$ and $q(x, \delta)$ are monomials, $f(x, \delta)$ is an affine function and $r(x, \delta)$ is an arbitrary polynomial in x and δ (it can be 1 as well). The resulting variables are: $B^{(1)}$, $\mathcal{N}_{\pi_b}^{(1)}(x, \delta)$, $\pi^{(1)}$. As the following example will show, this transformation can introduce several repetitive elements in $\pi^{(1)}$:

$$\underbrace{\begin{bmatrix} a & b \\ c & d \end{bmatrix}}_{B^{(0)}} \underbrace{\begin{bmatrix} x_2 + 2x_1^2 \\ x_2 \end{bmatrix}}_{\pi^{(0)}} = \underbrace{\begin{bmatrix} a & 2a & b \\ c & 2c & d \end{bmatrix}}_{B^{(1)}} \underbrace{\begin{bmatrix} x_2 \\ x_1^2 \\ x_2 \end{bmatrix}}_{\pi^{(1)}} \quad (3.3)$$

but the next algebraic step will resolve this problem.

3.2 Eliminating repetitive terms

As mentioned previously, the same monomials (or rational term with monomial numerator) can appear several times in $\pi^{(1)}$. In Section 3.7, I made a detailed study on the dimension of the optimization problem and how these are influenced by the sizes of π_b and the annihilators. After that analysis, I found that eliminating the repetitive terms in $\pi^{(1)}$ will lead to a significant dimension reduction of the computational problem. In order to keep the model equations, the corresponding columns in $B^{(1)}$ and $\mathcal{N}_{\pi_b}^{(1)}(x, \delta)$ shall be merged in the following way:

$$\underbrace{\begin{bmatrix} a(x, \delta) & b(x, \delta) \end{bmatrix}}_{\text{left multiplier}} \underbrace{\begin{bmatrix} \alpha p(x, \delta) \\ \beta p(x, \delta) \end{bmatrix}}_{\pi^{(1)}} = \underbrace{\begin{bmatrix} \alpha a(x, \delta) + \beta b(x, \delta) \end{bmatrix}}_{\text{modified left multipliers}} \underbrace{\begin{bmatrix} p(x, \delta) \end{bmatrix}}_{\pi^{(2)}} \quad (3.4)$$

The resulting variables will be: $B^{(2)}$, $\mathcal{N}_{\pi_b}^{(2)}(x, \delta)$, $\pi^{(2)}$. Considering example (3.3) from the the previous section, the final model will be:

$$\underbrace{\begin{bmatrix} a & 2a & b \\ c & 2c & d \end{bmatrix}}_{B^{(1)}} \underbrace{\begin{bmatrix} x_2 \\ x_1^2 \\ x_2 \end{bmatrix}}_{\pi^{(1)}} = \underbrace{\begin{bmatrix} a+b & 2a \\ c+d & 2c \end{bmatrix}}_{B^{(2)}} \underbrace{\begin{bmatrix} x_2 \\ x_1^2 \end{bmatrix}}_{\pi^{(2)}} \quad (3.5)$$

$B^{(2)}$ and $\pi^{(2)}$ constitutes the final values of B and π , therefore, the superscripts will be suppressed in the sequel, but the annihilator $\mathcal{N}_{\pi_b}^{(2)}(x, \delta)$ will require further modifications.

3.3 Annihilator generation

As mentioned previously, the annihilator plays an important role in the optimization problem by making the conditions less conservative. Using annihilators, the algebraic relations between the dependent variables of the model can be taken into consideration by the solver. The main objective in searching for an adequate annihilator is, to find as many independent annihilator rows as possible, in order to exploit the possible degrees of freedom of the computational problem, therefore, further rows will be appended to the existing annihilator $\mathcal{N}_{\pi_b}^{(2)}(x, \delta)$.

Using Matlab's symbolic toolbox, I have written an algorithm, which can generate affine annihilator rows of a special form.

If π_b contains only monomials (no rational terms), then it is enough if in each row of the matrix there appear only two nonzero items because, if an element $p_k(x, \delta)$ of π_b can be eliminated by some other elements $p_i(x, \delta)$, for every i chosen from an given index set \mathcal{I}_k , i.e.

$$\begin{aligned} \exists a, b_i : \mathcal{X} \times \mathcal{D} \mapsto \mathbb{R}, \quad i \in \mathcal{I}_k, \quad \text{affine functions of } (x, \delta) \\ \text{s.t. } p_k(x, \delta)a(x, \delta) + \sum_{i \in \mathcal{I}_k} p_i(x, \delta)b_i(x, \delta) = 0 \end{aligned} \quad (3.6)$$

then $p_k(x, \delta)$ can be eliminated by only a single element arbitrarily chosen from $p_i(x, \delta)$, in other words

$$\begin{aligned} \forall i \in \mathcal{I}_k \quad \exists \bar{a}, \bar{b} : \mathcal{X} \times \mathcal{D} \mapsto \mathbb{R}, \quad \text{affine monomials} \\ \text{s.t. } p_k(x, \delta)\bar{a}(x, \delta) + p_i(x, \delta)\bar{b}(x, \delta) = 0 \end{aligned} \quad (3.7)$$

This statement is no longer valid when there are further rational terms with monomial numerator. Consider the following simple example. If $\pi_b = \begin{bmatrix} x & \frac{1}{x^2+1} & \frac{x^2}{x^2+1} \end{bmatrix}^T$, then there exists an affine annihilator row $r(x) = \begin{bmatrix} -1 & x & x \end{bmatrix}$, such that $r(x)\pi_b = 0$. However, if we chose two arbitrary elements from π_b , their linear combination with affine coefficients

will never be zero. Fortunately, the LFT can produce a few such rows in $\mathcal{N}_{\pi_b}^{(0)}(x, \delta)$, that they fulfill the extra relations between elements of π_b having different denominators. Therefore, I assume that it is enough if in each row only two nonzero items appear, which eliminate the two corresponding elements in π_b . In my algorithm, I search for annihilator rows of the following form:

$$\begin{bmatrix} \cdots & \alpha x_i & \cdots & \beta x_j & \cdots \\ \cdots & \alpha x_i & \cdots & \beta & \cdots \\ \cdots & \alpha & \cdots & \beta x_j & \cdots \end{bmatrix} \quad (3.8)$$

I chose two elements from π_b , let them be $p_i(x, \delta)$, $p_j(x, \delta)$, where $i < j$. If the numerator $b(x, \delta)$ and the denominator $a(x, \delta)$ of their simplified fraction $\frac{p_i(x, \delta)}{p_j(x, \delta)} \left(= \frac{b(x, \delta)}{a(x, \delta)} \right)$ are affine monomials, then a new *affine* row can be appended to the annihilator:

$$r(x, \delta) = [\dots \underbrace{a(x, \delta)}_{i\text{th element}} \dots \underbrace{-b(x, \delta)}_{j\text{th element}} \dots]$$

since $p_i(x, \delta)a(x, \delta) - p_j(x, \delta)b(x, \delta) = 0$. This procedure is evaluated on each pair of the elements of π_b .

“Advantageous” annihilator

It is clear from the problem definition that the annihilator corresponding to a given Lyapunov function computation is non-unique, but there are no results in the literature, how to construct a “good” annihilator. In this section, $N(x, \delta)$ will denote an arbitrary annihilator of a given $\pi_b : \mathbb{R}^n \times \mathcal{D} \mapsto \mathbb{R}^m$ rational mapping. It is not straightforward to clearly define which annihilator can be considered as the “best one”, because many things depend upon the annihilators during the operation of the optimization procedure. It is a fact that the maximum number of linearly independent rows (in the meaning of classical matrix theory) in $N(x, \delta)$ is $m - 1$, because $\pi_b \in \mathbb{R}^m$, however, it is demonstrated in Example 3. that using an annihilator containing more rows than this maximal rank may result in a less conservative condition, since it can introduce more independent decision variables in the optimization problem.

Example 3. This example is borrowed from [1], characterized by equations (5,7,9,12,13). Let us consider a third order system $\dot{x} = A(x)x$, where

$$A(x) = \begin{bmatrix} x_2 + x_3 - 1 & 1 - x_2 & x_2 - x_3 \\ -x_1 - 1 & x_1 + x_3 - 1 & 1 \\ -x_1 - x_2 & -x_2 - 1 & x_1 - 1 \end{bmatrix} \quad (3.9)$$

Let us choose a quadratic Lyapunov function $V(x) = x^T P x$ with a symmetric positive

definite matrix P . Note that this form of the Lyapunov function is a special case of (2.7), when $\pi_b = x$. Its time derivative is: $\dot{V}(x) = x^T(A^T(x)P + PA(x))x$. According to Finsler's lemma, if the LMI

$$A^T(x)P + PA(x) + LN(x) + N^T(x)L^T \leq 0, \quad \forall x \in \vartheta(\mathcal{X}) \quad (3.10)$$

is satisfied, then $\dot{V}(x)$ is negative for every $x \in \mathcal{X}$. In equation (3.10), the matrix function $N(x)$ is an affine annihilator of x . In this inequality, the P and L are free parameters of the semidefinite problem (SDP), furthermore, the number of decision variables in L is equal with the number of elements of annihilator $N(x)$.

I define a polytope $\mathcal{X} = \{x : |x_i| \leq \beta, x_i \in \mathbb{R}\}$, on which the inequality will be tested. The area of this polytope can be arbitrarily chosen by modifying the value of the parameter β . Then, I demonstrate four different annihilators $N_i(x), i = \overline{1,4}$ and find out which of them results in the least conservative condition, in other words, I try to solve the LMI for larger and larger polytopes (by gradually increasing the value of β), and approximate its maximal value β_{max} while the LMI is still feasible. The least conservative LMI corresponds to the highest β_{max} value. The annihilators and the corresponding maximal β values are listed in the following equations.

$$\begin{aligned} N_1(x) &= \begin{bmatrix} x_2 & -x_1 & 0 \\ 0 & x_3 & -x_2 \end{bmatrix} & \beta_{max} &= 0.9296 \\ N_2(x) &= \begin{bmatrix} x_2 & -x_1 & 0 \\ x_3 & 0 & -x_1 \end{bmatrix} & \beta_{max} &= 1 \\ N_3(x) &= \begin{bmatrix} 0 & x_3 & -x_2 \\ x_3 & 0 & -x_1 \end{bmatrix} & \beta_{max} &= 0.71418 \\ N_4(x) &= \begin{bmatrix} x_2 & -x_1 & 0 \\ x_3 & 0 & -x_1 \\ 0 & x_3 & -x_2 \end{bmatrix} & \beta_{max} &= 560102.3 \end{aligned} \quad (3.11)$$

One can observe that the rows of $N_4(x)$ are linearly dependent, since the second row can be expressed by the first and the third rows:

$$\frac{x_3}{x_1} \begin{bmatrix} x_2 & -x_1 & 0 \end{bmatrix} + \frac{x_1}{x_2} \begin{bmatrix} 0 & x_3 & -x_2 \end{bmatrix} = \begin{bmatrix} x_3 & 0 & -x_1 \end{bmatrix} \quad (3.12)$$

In the same time, annihilator $N_4(x)$ produces the least conservative inequality condition, because it involves more independent decision variables into the problem. This example clearly demonstrates that annihilator $N_4(x)$ is a "better" annihilator than the first three annihilators, even though, its rows are linearly dependent.

3.4 Finding an appropriate Lyapunov function

After the previous steps, I consider a model (2.11). A Lyapunov function candidate for this system is given in the form $V(x, \delta) = x^T \mathbf{P}(x, \delta)x = \pi_b^T P \pi_b$ (3.13), where $P \in \mathbb{R}^{m \times m}$ is a constant symmetric matrix. As it has been mentioned in Section 2.3, the positive definiteness of $V(x, \delta)$ can be expressed by a stricter inequality:

$$\begin{aligned} \exists L_b \in \mathbb{R}^{m \times q}, \quad \text{such that:} \\ P + L_b \mathcal{N}_{\pi_b}(x, \delta) + \mathcal{N}_{\pi_b}^T(x, \delta) L_b^T > 0, \quad \forall (x, \delta) \in \vartheta(\mathcal{X} \times \mathcal{D}) \end{aligned} \quad (3.14)$$

The negative definiteness of $\dot{V}(x, \delta, \dot{\delta}) = \nabla V(x, \delta) \dot{x}$ is ensured by the following sufficient LMI condition:

$$\begin{aligned} \exists L_a \in \mathbb{R}^{(n+2p+n^2+np) \times (2q+n^2+nq)}, \quad \text{such that:} \\ P_a + P_a^T + L_a \mathcal{N}_{\pi_a}(x, \delta, \dot{\delta}) + \mathcal{N}_{\pi_a}^T(x, \delta, \dot{\delta}) L_a^T < 0, \quad \forall (x, \delta, \dot{\delta}) \in \vartheta(\mathcal{X} \times \mathcal{D} \times \check{\mathcal{D}}), \end{aligned} \quad (3.15)$$

where the matrix P_a is defined as:

$$P_a = \begin{bmatrix} P A_a \\ 0_{(p+n^2+np) \times (n+2p+n^2+np)} \end{bmatrix} \quad A_a = \begin{bmatrix} A & B & 0_{n \times p} & 0_{n \times (n^2+np)} \\ 0_{p \times n} & 0_{p \times p} & I_p & 0_{p \times (n^2+np)} \end{bmatrix} \quad (3.16)$$

In order to define the annihilator $\mathcal{N}_{\pi_a}(x, \delta, \dot{\delta})$, some auxiliary variables are needed to be introduced:

$$\begin{aligned} \bar{E}_k &= \text{row}_k(I_n) \\ E_0(x) &= [x \bar{E}_k]_{\text{col}}^{k=\overline{1, n}} = I_n \otimes x \in \mathbb{R}^{n^2 \times n} \\ E_1(x, \delta) &= [\pi \bar{E}_k]_{\text{col}}^{k=\overline{1, n}} = I_n \otimes \pi \in \mathbb{R}^{np \times n} \end{aligned} \quad \begin{aligned} J_0 &= \begin{bmatrix} I_n \\ 0_{p \times n} \end{bmatrix} \\ J_1 &= \begin{bmatrix} 0_{n \times p} \\ I_p \end{bmatrix} \end{aligned} \quad (3.17)$$

It is worth mentioning that $E_0(x)$ is an affine matrix function of x , while $E_1(x, \delta)$ is a rational function of (x, δ) due to its entries are borrowed from π . The affine annihilator $\mathcal{N}_{\pi_b}(x, \delta)$ of π_b is decomposed as follows:

$$\mathcal{N}_{\pi_b}(x, \delta) = H_0 + \bar{H}(x) + \hat{H}(\delta) \quad (3.18)$$

$$\bar{H}(x) = \sum_{k=1}^n \bar{H}_k x_k, \quad \hat{H}(\delta) = \sum_{k=1}^d \hat{H}_k \delta_k, \quad \hat{H}(\dot{\delta}) = \sum_{k=1}^d \hat{H}_k \dot{\delta}_k \quad (3.19)$$

where x_k, δ_k are elements of x and δ , respectively. By using the constant matrices $H_0, \bar{H}_k, \hat{H}_k$, the following variables are constructed:

$$\begin{aligned}\bar{M}_\mu &= [\bar{H}_k J_0]_{\text{row}}^{k=\overline{1,n}} \in \mathbb{R}^{q \times n^2} & M_\mu(x, \delta) &= I_n \otimes \mathcal{N}_{\pi_b}(x, \delta) J_0 \in \mathbb{R}^{qn \times n^2} \\ \bar{M}_\eta &= [\bar{H}_k J_1]_{\text{row}}^{k=\overline{1,n}} \in \mathbb{R}^{q \times np} & M_\eta(x, \delta) &= I_n \otimes \mathcal{N}_{\pi_b}(x, \delta) J_1 \in \mathbb{R}^{qp \times np}\end{aligned}\quad (3.20)$$

$$W(x, \delta, \dot{\delta}) = \hat{H}(\dot{\delta}) + \mathcal{N}_{\pi_b}(x, \delta) J_0 [A \ B] \quad (3.21)$$

Due to the properties of $\mathcal{N}_{\pi_b}(x, \delta)$, the matrix functions M_μ and M_η are affine in (x, δ) , furthermore, $W(x, \delta, \dot{\delta})$ is an affine matrix function of $(x, \delta, \dot{\delta})$. Finally, one can construct the following object:

$$\mathcal{N}_{\pi_a}(x, \delta, \dot{\delta}) = \begin{bmatrix} \mathcal{N}_{\pi_b}(x, \delta) & 0_{q \times p} & 0_{q \times n^2} & 0_{q \times np} \\ W(x, \delta, \dot{\delta}) & \mathcal{N}_{\pi_b}(x, \delta) J_1 & \bar{M}_\mu & \bar{M}_\eta \\ E_0(x) [A \ B] & 0_{n^2 \times p} & -I_{n^2} & 0_{n^2 \times np} \\ 0_{nq \times m} & 0_{nq \times p} & M_\mu(x, \delta) & M_\eta(x, \delta) \end{bmatrix} \quad (3.22)$$

\mathcal{N}_{π_a} is an $(2q + n^2 + nq) \times (n + 2p + n^2 + np)$ affine matrix function of $(x, \delta, \dot{\delta})$ and it is the annihilator of $\pi_a(x, \delta, \dot{\delta}) = [\pi_b, \dot{\pi}, \mu, \eta]_{\text{col}}$, which appears in the derivative of the Lyapunov function (3.13):

$$\dot{V}(x, \delta, \dot{\delta}) = \pi_a^T (P_a + P_a^T) \pi_a \quad (3.23)$$

The latter two artificial variables in $\pi_a = \pi_a(x, \delta, \dot{\delta})$ are defined as:

$$\begin{aligned}\mu_k &= \mu_k(x) \stackrel{\text{def}}{=} x \dot{x}_k, & \mu &= [\mu_k]_{\text{col}}^{k=\overline{1,n}} = E_0(x) \dot{x} \in \mathbb{R}^{n^2} \\ \eta_k &= \eta_k(x, \delta) \stackrel{\text{def}}{=} \pi \dot{x}_k, & \eta &= [\eta_k]_{\text{col}}^{k=\overline{1,n}} = E_1(x, \delta) \dot{x} \in \mathbb{R}^{np}\end{aligned}\quad (3.24)$$

In comparison with the formulas presented in [1], in the definition of the μ there appear a difference in its sign, fortunately in the expression of $\dot{V}(x, \delta, \dot{\delta})$ the μ is multiplied by zeros, therefore, P_a can remain the same, furthermore, the affine matrix function $\mathcal{N}_{\pi_a}(x, \delta, \dot{\delta})$ is constructed by merging the two annihilators $C_a(x, \delta, \dot{\delta})$ and $\aleph_{\pi_a}(x, \delta, \dot{\delta})$, keeping in mind that sign of μ was changed. The previous two matrix functions C_a and \aleph_{π_a} are defined in [1] by equations (40,43).

Derivation of $\mathcal{N}_{\pi_a}(x, \delta, \dot{\delta})$

It is trivial that the first row of $\mathcal{N}_{\pi_a}(x, \delta, \dot{\delta})$ is indeed an annihilator of π_a . The second row is constructed by using the expansion of the time derivative of the equality $\mathcal{N}_{\pi_b}(x, \delta) \pi_b = 0$, that is

$$\frac{d\mathcal{N}_{\pi_b}(x, \delta) \pi_b}{dt} = \frac{d\mathcal{N}_{\pi_b}(x, \delta) J_0 x}{dt} + \frac{\mathcal{N}_{\pi_b}(x, \delta) J_1 \pi}{dt} = 0. \quad (3.25)$$

After computing the derivatives entrywise, one can get

$$\dot{\mathcal{N}}_{\pi_b}(x, \delta)J_0x + \mathcal{N}_{\pi_b}(x, \delta)J_0\dot{x} + \dot{\mathcal{N}}_{\pi_b}(x, \delta)J_1\pi + \mathcal{N}_{\pi_b}(x, \delta)J_1\dot{\pi} = 0. \quad (3.26)$$

As presented in equation (3.18), the annihilator $\mathcal{N}_{\pi_b}(x, \delta)$ can be decomposed as the sum of the objects H_0 , $\bar{H}(x)$ and $\hat{H}(\delta)$, then the equality will look like

$$\bar{H}(\dot{x})J_0x + \hat{H}(\dot{\delta})J_0x + \mathcal{N}_{\pi_b}(x, \delta)J_0[A \ B]\pi_b + \bar{H}(\dot{x})J_1\pi + \hat{H}(\dot{\delta})J_1\pi + \mathcal{N}_{\pi_b}(x, \delta)J_1\dot{\pi} = 0$$

Using the expression of matrix functions $\bar{H}(x)$ and $\hat{H}(\delta)$, one can obtain

$$\underbrace{\left(\hat{H}(\dot{\delta}) + \mathcal{N}_{\pi_b}(x, \delta)J_0[A \ B]\right)}_{W(x, \delta, \dot{\delta})} \pi_b + \mathcal{N}_{\pi_b}(x, \delta)J_1\dot{\pi} + \sum_{k=1}^n \bar{H}_k J_0 \mu_k + \sum_{k=1}^n \bar{H}_k J_1 \eta_k = 0 \quad (3.27)$$

from which the final form of the second row can be obtained.

The third row of $\mathcal{N}_{\pi_a}(x, \delta, \dot{\delta})$ is coming from the fact that $\mu = E_0(x)\dot{x} = E_0(x)[A \ B]\pi_b$. Regarding the fourth row, one shall note, that $[M_\mu(x, \delta) \ M_\eta(x, \delta)]$ is an annihilator of $[\mu, \eta]_{\text{col}}$, because

$$M_\mu(x, \delta)\mu + M_\eta(x, \delta)\eta = 0 \quad (3.28)$$

In order to prove this equality, we should evaluate the left hand side of equation (3.28). Replacing variables μ and η by their definitions introduced in equations (3.24), the obtained form is:

$$M_\mu(x, \delta)E_0(x)\dot{x} + M_\eta(x, \delta)E_1(x, \delta)\dot{x} \quad (3.29)$$

After substituting the matrices M_μ , M_η , $E_0(x)$ and $E_1(x, \delta)$ with their definitions, the expression (3.29) develops into the form:

$$(I_n \otimes \mathcal{N}_{\pi_b}(x, \delta)J_0)(I_n \otimes x)\dot{x} + (I_n \otimes \mathcal{N}_{\pi_b}(x, \delta)J_1)(I_n \otimes \pi)\dot{x} \quad (3.30)$$

Since the Kronecker product is distributive with respect to the addition and matrix multiplication, we can pull out the Kronecker product operation to the front of the equation:

$$\left(I_n \otimes \left(\mathcal{N}_{\pi_b}(x, \delta)J_0x + \mathcal{N}_{\pi_b}(x, \delta)J_0\pi\right)\right)\dot{x} \quad (3.31)$$

Using the definitions of J_0 and J_1 and then evaluating the inner sum, one can make certain, that the expression (3.28) is indeed the zero vector: $(I_n \otimes \mathcal{N}_{\pi_b}(x, \delta)\pi_b)\dot{x} = 0 \in \mathbb{R}^{nm \times 1}$. For details, see Theorem 4.1 in [1, Section 4].

3.5 Finding the maximal level set for a given polytope

My solution for finding the maximal level set of Lyapunov functions is based on two popular approaches from the literature. The differences between the methods proposed in [19] and [1] are related to the definition of the sets, on which the conditions are stated, and the objective function, which is used to maximize the size of the invariant region.

1. Topcu required the Lyapunov function to be positive definite on the whole \mathbb{R}^n but the function's time derivative should be negative definite only in the inside of the level set ε , which would be the final invariant level set as it reaches its maximal size (Lemma 1. in [19]). In order to maximize the size of ε , Topcu defined a region $\mathcal{P}_\beta = \{x \in \mathbb{R}^n \mid p(x) \leq \beta\}$, which should lie inside ε , while the variable β is maximized. The polynomial $p(x)$ is a design factor, which determines the shape and the orientation of the inner region.
2. On the other hand, in [1] the authors do not prescribe any constraint outside a given polytopic set $\mathcal{X} \subset \mathbb{R}^n$, but for every $x \in \mathcal{X}$ the Lyapunov function and its derivative is required to be positive and negative definite, respectively. Furthermore, an additional constraint is introduced, namely the level set $\varepsilon_1 = \{x \in \mathbb{R}^n \mid V(x) = 1\}$ should lie in the inside of the polytope \mathcal{X} . In this case, the objective function to be minimized is the sum of values of the Lyapunov function in some points $x \in \mathcal{X}$, which are strategically chosen. Such an objective function can ensure that the level set $V(x) = 1$ is as close to the boundary of \mathcal{X} as possible.

In order to find the maximal invariant level set, I adopted a combined method of these two techniques. First of all, I defined a small polytope \mathcal{Y} around the locally stable origin inside \mathcal{X} . Similarly to the first approach, the size of the polytope \mathcal{Y} can depend on a parameter and can be maximized, producing a maximal level set around \mathcal{Y} . The challenge is that the matrix inequality conditions are no longer linear using this approach, hence the need arises for further relaxations.

Instead, I define the polytope $\mathcal{Y} \subset \mathcal{X}$ to have a small but constant size, looking for a level set $\varepsilon_\alpha = \{x \in \mathcal{X} \mid V(x) = \alpha, 1 \leq \alpha\}$ that is inside of \mathcal{X} , while ε_1 is outside of \mathcal{Y} . Then, I have to maximize α , under the conditions

1. ε_α lies in the inside of \mathcal{X}
2. \mathcal{Y} is inside ε_1 (without this condition the function $V(x)$ can be scaled arbitrarily leading to an unbounded optimum).

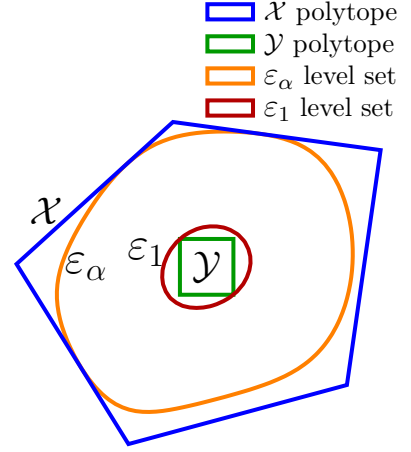


Figure 3.1

Transforming into LMI conditions

The first condition is satisfied if the value of the Lyapunov function is greater than α along the boundary of \mathcal{X} (denoted by $\partial\mathcal{X}$). Formally:

$$V(x, \delta) = \pi_b^T P \pi_b \geq \alpha \quad \forall \delta \in \mathcal{D}, \forall x \in \partial\mathcal{X} \quad (3.32)$$

It is obvious that $\partial\mathcal{X}$ is not a convex set, but it can be obtained as the union of the facets of \mathcal{X} , which are indeed convex ($n - 1$ dimensional) manifolds (see Figure 3.2). Therefore, the same condition is tested several times for each facet of \mathcal{X} , which are converted into LMI conditions. First of all, let me introduce some auxiliary notations:

- $\mathcal{F}_k^{(\mathcal{X})}$ is the k th facet of \mathcal{X} , where $k = \overline{1, M_{\mathcal{X}}}$, $M_{\mathcal{X}}$ is the number of facets of \mathcal{X} ,
- d_k is the distance of facet $\mathcal{F}_k^{(\mathcal{X})}$ from the origin,
- n_k is a normal vector orthogonal to facet $\mathcal{F}_k^{(\mathcal{X})}$ pointing towards $\mathcal{F}_k^{(\mathcal{X})}$, (Figure 3.2, red arrows)
- Finally the vector $a_k = \frac{n_k}{d_k}$ satisfies $\mathcal{F}_k^{(\mathcal{X})} \subset \{x : \langle a_k, x \rangle = 1\}$.

With the intention of demonstration, Figure 3.2 illustrates that an arbitrary point $x \in R^n$ is an element of \mathcal{X} if $\langle n_k, x \rangle \leq d_k$, equivalently, if $\langle a_k, x \rangle \leq 1$ for all $k = \overline{1, M_{\mathcal{X}}}$.

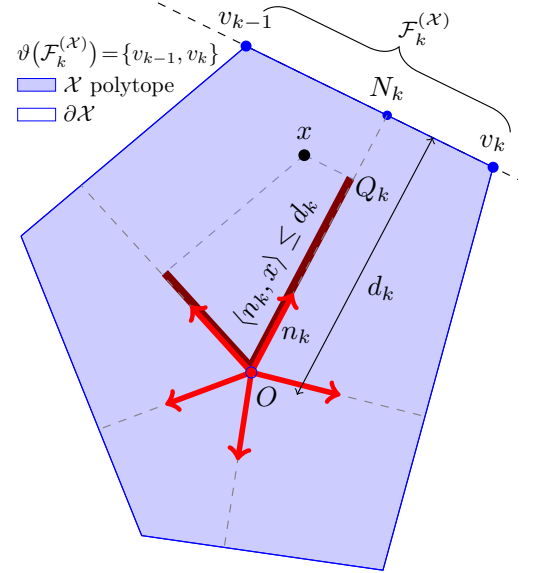


Figure 3.2

Using the notations, the inequality (3.32) can be reformulated as:

$$\forall k = \overline{1, M_{\mathcal{X}}} : V(x, \delta) - \alpha = \pi_c^T \begin{bmatrix} P & 0 \\ 0 & -\alpha \end{bmatrix} \pi_c \geq 0 \quad \forall \delta \in \mathcal{D}, \forall x \in \mathcal{F}_k^{(\mathcal{X})} \quad (3.33)$$

$$\text{where } \pi_c = \begin{bmatrix} \pi_b \\ 1 \end{bmatrix} \in \mathbb{R}^{m+1}$$

Similarly to [1], further notations are introduced:

$$\begin{aligned} C_0 &= [I_n \ 0_{n \times p}] \in \mathbb{R}^{n \times m} & \mathcal{N}_{\pi_c}(x, \delta) &= [C_0 \ -x] \in \mathbb{R}^{n \times (m+1)} \\ C_k &= [a_k^T C_0 \ -1] \in \mathbb{R}^{1 \times (m+1)} & Q_k &= \begin{bmatrix} I_m \\ a_k^T C_0 \end{bmatrix} \in \mathbb{R}^{(m+1) \times m} \end{aligned} \quad (3.34)$$

Observe that $C_0 \pi_b = x$ and $\mathcal{N}_{\pi_c}(x, \delta) \pi_c = 0$ for all $x \in \mathbb{R}^n$. Furthermore, knowing that $x \in \mathcal{F}_k^{(\mathcal{X})} \subset \{x : a_k^T x = 1\}$ follows that $a_k^T C_0 \pi_b - 1 = C_k \pi_c = 0$ but only for $x \in \mathcal{F}_k^{(\mathcal{X})}$ (and not for every $x \in \mathbb{R}^n$), therefore the constant matrix C_k can be considered as an annihilator of π_c , which describes the extra properties of x regarding to the fact that x is an element of $\mathcal{F}_k^{(\mathcal{X})}$. On the other hand, $C_k Q_k = 0_{1 \times m}$, consequently, the columns of Q_k span the null-space of C_k .

Two more matrix functions are defined as:

$$R_k(x, \delta) = \begin{bmatrix} L_{c_k} \mathcal{N}_{\pi_b}(x, \delta) + \mathcal{N}_{\pi_b}^T(x, \delta) L_{c_k}^T & 0_{m \times 1} \\ 0_{1 \times m} & 0_{1 \times 1} \end{bmatrix} + M_{c_k} \mathcal{N}_{\pi_c}(x, \delta) + \mathcal{N}_{\pi_c}(x, \delta)^T M_{c_k}^T \quad (3.35)$$

$$P_{c_k}^{(\alpha)}(x, \delta) = \begin{bmatrix} P & 0 \\ 0 & -\alpha \end{bmatrix} + R_k(x, \delta) \quad (3.36)$$

It is important to mention that $P_{c_k}^{(\alpha)}(x, \delta)$ is an affine matrix function in x and δ . The identities $\mathcal{N}_{\pi_b}(x, \delta) \pi_b = 0_{q \times 1}$ and $\mathcal{N}_{\pi_c}(x, \delta) \pi_c = 0_{n \times 1}$ for all $(x, \delta) \in \mathcal{X} \times \mathcal{D}$ imply that $\pi_c^T R_k(x, \delta) \pi_c = 0$ for all $(x, \delta) \in \mathcal{X} \times \mathcal{D}$. To conclude, a sufficient condition for (3.33) can be formulated:

$$\forall k = \overline{1, M_{\mathcal{X}}} : \pi_c^T P_{c_k}^{(\alpha)}(x, \delta) \pi_c \geq 0 \quad \forall \delta \in \mathcal{D}, \forall x \in \mathcal{F}_k^{(\mathcal{X})} \quad (3.37)$$

With reference to the equivalence of (i) and (iii) in Finsler's lemma, and using that $C_k \pi_c = 0$ for all $x \in \mathcal{F}_k^{(\mathcal{X})}$, where C_k has a null-space Q_k , (3.37) is equivalent to the following LMI:

$$\begin{aligned} \forall k = \overline{1, M_{\mathcal{X}}} : \exists L_{c_k} \in \mathbb{R}^{m \times q}, \exists M_{c_k} \in \mathbb{R}^{(m+1) \times n}, \text{ such that:} \\ Q_k^T P_{c_k}^{(\alpha)}(x, \delta) Q_k \geq 0, \quad \forall (x, \delta) \in \vartheta(\mathcal{F}_k^{(\mathcal{X})} \times \mathcal{D}), \end{aligned} \quad (3.38)$$

In the same way, the second condition (\mathcal{Y} lies in the inside of ε_1) can be formulated as:

$$\begin{aligned} \forall k = \overline{1, M_{\mathcal{Y}}} : \quad & \exists \bar{L}_{c_k} \in \mathbb{R}^{m \times q}, \quad \exists \bar{M}_{c_k} \in \mathbb{R}^{(m+1) \times n}, \quad \text{such that:} \\ & \bar{Q}_k^T \bar{P}_{c_k}^{(1)}(x, \delta) \bar{Q}_k \leq 0, \quad \forall (x, \delta) \in \vartheta(\mathcal{F}_k^{(\mathcal{Y})} \times \mathcal{D}), \end{aligned} \quad (3.39)$$

Finally, the optimization problem to find an appropriate Lyapunov function and its maximal invariant level set completely inside of the given polytope \mathcal{X} becomes:

$$\min_{1 \leq \alpha} (-\alpha) \quad \text{s.t. (3.14), (3.15), (3.38), (3.39)} \quad (3.40)$$

3.6 Finding the most appropriate outer polytope

I used an iterative procedure in order to find the most suitable polytope \mathcal{X} , in which the Lyapunov conditions could be satisfied. The basic idea is to choose an initial polytope $\mathcal{X}^{(0)}$, which satisfies the LMI conditions, then enlarge it iteratively to obtain $\mathcal{X}^{(k)}$. In each iteration step the maximal level set $\varepsilon_{\alpha}^{(k)}$ is found, then a larger polytope $\mathcal{X}^{(k+1)}$ defined considering the shape of $\varepsilon_{\alpha}^{(k)}$. One possible solution can be to choose some uniformly distributed discrete points lying on level set $\varepsilon_{\alpha}^{(k)}$. These points span a polytope, which should be enlarged by a given increment, without changing its shape (practically, the coordinates of every corner point are multiplied by an $1 < \gamma \ll 2$ scalar factor).

A similar iteration can be applied, when constraining the polytope \mathcal{X} to be rectangular. This assumption can be very advantageous during the analysis of a higher (n th) order system, because \mathcal{X} has 2^n corner points

This iteration is also convenient during the analysis of dynamical systems with a significantly asymmetric DOA. In such cases, the corner points of \mathcal{X} were chosen manually.

3.7 Dimensions of the optimization problem

In this section, I want to illustrate quantitatively the dimensions of the optimization problem. The number of decision variables of each free matrix variable are the following:

matrix var.	number of decision variables	
α	1	
P	$\frac{1}{2}m(m+1)$	
L_b	mq	(3.41)
L_a	$(n+2p+n^2+np)(2q+n^2+nq)$	
L_{c_k} and \bar{L}_{c_k}	$(M_{\mathcal{X}} + M_{\mathcal{Y}}) \times mq$	
M_{c_k} and \bar{M}_{c_k}	$(M_{\mathcal{X}} + M_{\mathcal{Y}}) \times (m+1)n$	

Consequently, the number of decision variables of the whole computation procedure is the sum of the previous items. The formulas in equation (3.41) use the notations:

n : number of state parameters of the system (size of x)

p : number of elements in π

m : number of elements in π_b ($n+p$)

q : number of rows in the final $\mathcal{N}_{\pi_b}(x, \delta)$

$M_{\mathcal{X}}$: number of corner points of \mathcal{X}

$M_{\mathcal{Y}}$: number of corner points of \mathcal{Y}

Further important dimensional properties of the optimization problem are the number of LMIs and their sizes. These are presented in the next table:

eq. nr.	description	first dimension of the LMIs	nr of LMIs
(3.14)	positivity of $V(x, \delta)$	m	$M_{\mathcal{X}} \cdot M_{\mathcal{D}}$
(3.15)	negativity of $\dot{V}(x, \delta)$	$n+2p+n^2+np$	$M_{\mathcal{X}} \cdot M_{\mathcal{D}} \cdot M_{\dot{\mathcal{D}}}$
(3.38)	$V(x, \delta) \geq \alpha$ for all $x \in \partial\mathcal{X}$	$m+1$	$2 M_{\mathcal{X}} \cdot M_{\mathcal{D}}$
(3.39)	$V(x, \delta) \leq 1$ for all $x \in \partial\mathcal{Y}$	$m+1$	$2 M_{\mathcal{Y}} \cdot M_{\mathcal{D}}$

As one can observe, truncating π (decreasing p) reduces significantly the number of decision variables and the sizes of the LMIs, especially the LMIs corresponding to the derivative of the Lyapunov function. Not to mention the fact that, in general, a smaller π produces less rows (q) in the annihilator $\mathcal{N}_{\pi_b}(x, \delta)$.

4. Illustrative examples and results

In this chapter, I illustrate the applicability of the approach presented above through different numerical examples.

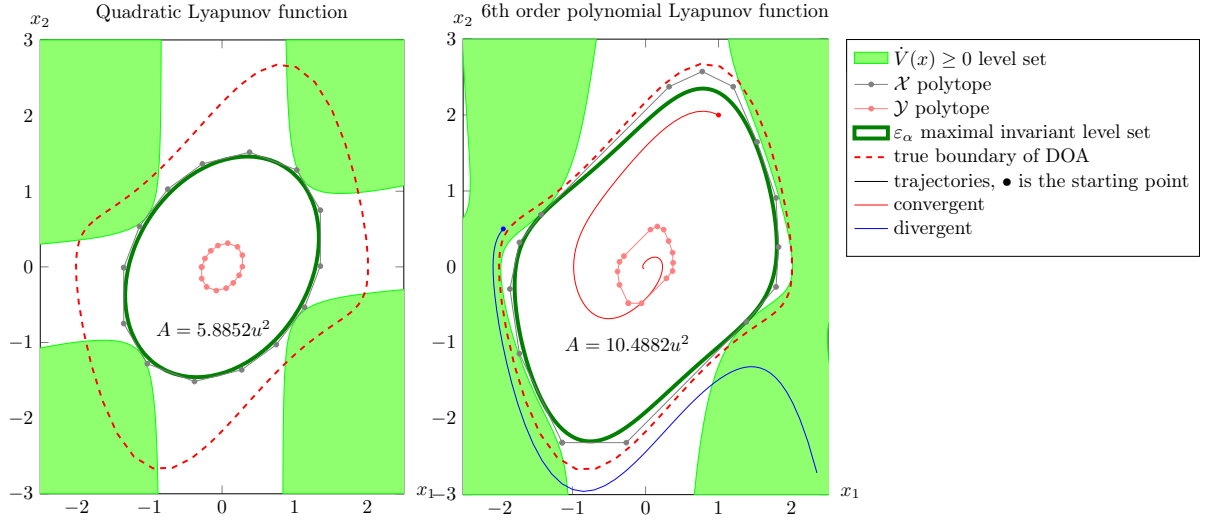
The results presented in this section have been computed in the Matlab environment. For symbolic computations, I used Matlab's built-in Symbolic Math Toolbox based on Mupad. For linear fractional transformations (LFT), I used the Enhanced LFR-toolbox [6, 5]. To model and solve semidefinite optimization (SDP) problems I used Mosek solver with YALMIP [8].

In each example the values of the following variables are given:

1. the generated column vector π containing the nonlinearities of the system,
2. the model matrices A, B and the annihilator $\mathcal{N}_{\pi_b}(x, \delta)$ appearing in equation (2.11),
3. the corner points $x^{(i)} \in \vartheta(\mathcal{X})$ of the final polytope \mathcal{X} . For the sake of simplicity, $\vartheta(\mathcal{X})$ is given in the following matrix form:

$$\vartheta(\mathcal{X}) = \left\{ x^{(i)} \mid i = \overline{1, M_{\mathcal{X}}} \right\} \rightarrow \begin{matrix} \left[\begin{array}{ccc} x_1^{(1)} & x_1^{(2)} & \dots \\ \dots & \dots & \dots \\ x_n^{(1)} & x_n^{(2)} & \dots \end{array} \right] \\ \text{“} \end{matrix} \quad (4.1)$$

4. the resulting matrix P of the Lyapunov function: $V(x, \delta) = \pi_b^T P \pi_b$ and the value of α . The variables of π, P and α uniquely determine the maximal invariant level set ε_α of the Lyapunov function: $\varepsilon_\alpha = \{x \in \mathcal{X} \mid V(x) = \pi_b^T P \pi_b = \alpha\}$. In case of uncertain systems, a robust invariant set is computed.
5. the area/volume (A/V) of the inner region bounded by ε_α , which is given in square units (u^2) and cubic units (u^3), respectively.



(a) The estimated DOA using a quadratic Lyapunov function (b) The generated DOA estimation using the algorithm presented in the previous chapters.

Figure 4.1: DOA estimation of the time inverted Van der Pol system

4.1 Van der Pol dynamics

The system

$$\begin{aligned} \dot{x}_1 &= -x_2 \\ \dot{x}_2 &= x_1 - \delta(1 - x_1^2)x_2 \quad \text{with } \delta = 1 \end{aligned} \tag{4.2}$$

describes a time-inverted oscillator introduced by the Dutch electrical engineer and physicist Balthasar van der Pol. This system has an asymptotically stable equilibrium point at the origin, and it has a limit cycle, which determines the boundary of the system's DOA. This limit cycle (dashed red line) and some trajectories (blue lines: not converging to the studied equilibrium point, red lines: converging to the equilibrium point) of the system can be seen in Figure 4.1, which also illustrates the maximal invariant level set (green line, right hand side) generated by the algorithm described in Chapter 3. The nonlinear monomials of π used in [1] were

$$\pi^T = [x_1^2 \quad x_1 x_2 \quad x_2^2 \quad x_1^3 \quad x_1^2 x_2 \quad x_1 x_2^2 \quad x_2^3] \tag{4.3}$$

In comparison, my approach generates a smaller number of monomials:

$$\pi^T = [x_1^2 x_2 \quad x_1 x_2] \tag{4.4}$$

The model matrices of (2.11) are:

$$A = \begin{bmatrix} 0 & -1 \\ 1 & -1 \end{bmatrix}, \quad B = \begin{bmatrix} 0 & 0 \\ 1 & 0 \end{bmatrix}, \quad \mathcal{N}_{\pi_b}(x) = \begin{bmatrix} 0 & 0 & 1 & -x_1 \\ 0 & x_1 & 0 & -1 \\ x_2 & 0 & 0 & -1 \\ x_2 & -x_1 & 0 & 0 \end{bmatrix} \quad (4.5)$$

The polytope \mathcal{X} was generated iteratively, then further corner points were added manually, which together comprise the final \mathcal{X} . The corner points of \mathcal{X} are:

$$\vartheta(\mathcal{X}) : \begin{bmatrix} -1.1428 & -0.2637 & 1.3806 & 1.7875 & 1.8223 & 1.7875 & 1.5278 & 1.2014 & \dots \\ -2.3149 & -2.3149 & -0.72525 & -0.2637 & 0.26138 & 0.9084 & 1.6456 & 2.3735 & \dots \\ \dots & 0.77679 & 0.3223 & -1.4321 & -1.7289 & -1.8591 & -1.7289 & -1.1428 & \\ \dots & 2.5733 & 2.3735 & 0.68844 & 0.3223 & -0.29084 & -1.1428 & -2.3149 \end{bmatrix} \quad (4.6)$$

The matrix P and the invariant level set ε_α obtained by my method are the following:

$$P = \begin{bmatrix} 5.961 & -4.3596 & 1.1176 & -0.033319 \\ -4.3596 & 5.0502 & -4.5011\text{E-}6 & -0.0073781 \\ 1.1176 & -4.5011\text{E-}6 & -0.057457 & 0.019362 \\ -0.033319 & -0.0073781 & 0.019362 & 0.25254 \end{bmatrix} \quad (4.7)$$

$$\varepsilon_\alpha = \{x \in \mathcal{X} \mid V(x) = \alpha = 17.4086\} \quad (4.8)$$

The area bounded by ε_α is $A = 10.4882u^2$. In comparison, the area of that obtained in [1] by using the first value of π in (4.3) was approximately $12.58u^2$. The area of the actual DOA is $13.6832u^2$. At the same time, the dimensions of the optimization problem are much smaller in case of π containing only two elements. In Section 3.7, it was presented in detail, how the number of the decision variables and the dimensions of the LMIs are affected by the number of elements in π . The solver's running time in case of my algorithm was approximately 0.5 seconds, whereas, the running time using the larger π in equation (4.3) was 15.16 seconds.

Quadratic Lyapunov function

Figure 4.1 also features a smaller DOA (bounded by green line in Figure 4.1a), which was obtained by the algorithm with the constraint that the Lyapunov function is quadratic. This was obtained by constraining P to the following form:

$$P = \begin{bmatrix} \bar{P}_{n \times n} & 0_{n \times p} \\ 0_{p \times n} & 0_{p \times p} \end{bmatrix}, \quad \bar{P}_{n \times n} \text{ is symmetric} \quad (4.9)$$

The generated Lyapunov function is quadratic in x :

$$\bar{P}_{n \times n} = \begin{bmatrix} 12.8311 & -3.0838 \\ -3.0838 & 10.7177 \end{bmatrix} \Rightarrow V(x) \simeq 13x_1^2 - \frac{31x_1x_2}{5} + 11x_2^2 \quad (4.10)$$

The maximal invariant level set is $\varepsilon_\alpha = \{x \in \mathcal{X} \mid V(x) = \alpha = 21.2364\}$, its area is $A = 5.8852u^2$. The final polytope \mathcal{X} was generated automatically by applying the iterative method presented in Section 3.6, and its corner points are:

$$\vartheta(\mathcal{X}) : \begin{bmatrix} -1.3522 & -1.3522 & -1.0276 & -0.37861 & 0.27043 & 0.74679 & 1.1358 & \dots \\ -9.9967\text{E-}3 & -0.74951 & -1.281 & -1.5157 & -1.3612 & -1.0276 & -0.53397 & \dots \\ \dots & 1.3522 & 1.3522 & 1.0276 & 0.37861 & -0.27043 & -0.74679 & -1.1358 & -1.3522 \\ \dots & 9.9967\text{E-}3 & 0.74951 & 1.281 & 1.5157 & 1.3612 & 1.0276 & 0.53397 & -9.9967\text{E-}3 \end{bmatrix} \quad (4.11)$$

4.2 Uncertain Van der Pol dynamics

Here, the classical time-inverted Van der Pol model (4.2) is considered with an uncertain parameter δ . The algorithm has generated the following model representation:

$$\pi = \begin{bmatrix} \delta x_2 \\ \delta x_1^2 x_2 \\ \delta x_1 x_2 \end{bmatrix}, \quad A = \begin{bmatrix} 0 & -1 \\ 1 & 0 \end{bmatrix}, \quad B = \begin{bmatrix} 0 & 0 & 0 \\ -1 & 1 & 0 \end{bmatrix} \quad (4.12)$$

$$\mathcal{N}_{\pi_b}(x, \delta) = \begin{bmatrix} 0 & 0 & 0 & 1 & -x_1 \\ 0 & 0 & x_1 & 0 & -1 \\ 0 & \delta & -1 & 0 & 0 \\ x_2 & -x_1 & 0 & 0 & 0 \end{bmatrix} \quad (4.13)$$

During my work, I have analysed three different types of uncertainty:

1. First of all, I assumed $\delta \in [\delta_{\min}, \delta_{\max}]$ to be an unknown constant parameter, therefore, its time derivative is zero. In the numerical calculations I used $\delta \in [1, 3]$. In Figure 4.2a, the limit cycle of the system is shown for three different values of δ . The area of the obtained invariant domain (bounded by the green line) is $A = 5.677u^2$. The generated matrix P of function $V(x, \delta)$ and the value of α are:

$$P = \begin{bmatrix} 15.2167 & -4.7641 & -0.42159 & 0.66543 & -0.0048827 \\ -4.7641 & 10.3229 & 0.054745 & 0.37397 & 0.041035 \\ -0.42159 & 0.054745 & 0.011178 & 8.015\text{E-}07 & -0.0067726 \\ 0.66543 & 0.37397 & 8.015\text{E-}07 & 0.023439 & -0.0053948 \\ -0.0048827 & 0.041035 & -0.0067726 & -0.0053948 & -0.24081 \end{bmatrix} \quad (4.14)$$

$$\alpha = 22.3339$$

Due to the fact that the uncertain parameter δ appears in the Lyapunov function, the maximal invariant level set depends on δ . In this case, the estimated *robust* DOA (meaning the domain that is attracting for any value of δ) is computed as the intersection of the bounded regions of the maximal invariant level sets for all possible values of δ :

$$\text{estimated robust DOA: } \varepsilon_\alpha^* = \bigcap_{\delta \in \mathcal{D}} \left\{ x \in \mathcal{X} \mid V(x, \delta) \leq \alpha \right\} \quad (4.15)$$

Equivalently, ε_α^* can be obtained as the bounded region of the α -level set of the function $V^*(x) = \max_{\delta \in \mathcal{D}} V(x, \delta)$, i.e.

$$\varepsilon_\alpha^* = \left\{ x \in \mathcal{X} \mid \alpha \geq V^*(x) = \max_{\delta \in \mathcal{D}} V(x, \delta) \right\} \quad (4.16)$$

This can be done, because for every $x_0 \in \bigcap_{\delta \in \mathcal{D}} \left\{ x \in \mathcal{X} \mid V(x, \delta) \leq \alpha \right\}$ it is true that $V(x_0, \delta) \leq \alpha$ for every δ in \mathcal{D} , therefore, $V(x_0, \delta) \leq \max_{\delta \in \mathcal{D}} V(x_0, \delta) \leq \alpha$. Computationally, this second approach in equation (4.16) is more advantageous to calculate the robust invariant region ε_α^* .

2. Secondly, I assumed $\delta = \delta(t)$ to be known, but it depends on time. In the computations, I used $\delta = a + b \sin(\omega t)$, therefore, the possible values of δ belong to the interval $\mathcal{D} = [a - b, a + b]$, while the time derivative of δ operates on the interval $\check{\mathcal{D}} = [-\omega b, \omega b]$. Figure 4.2b illustrates the approximated boundary of the DOA. The approximation was obtained by simulating the time-inverted system considering an initial state close to the origin. If (a, b, ω) are given the values $(1, 0.8, 10.5)$, the area of the estimated DOA is $A = 3.6226u^2$. The generated P and the value of α are:

$$P = \begin{bmatrix} 19.1483 & -1.7335 & -0.052569 & 0.061823 & -1.5114\text{E-}06 \\ -1.7335 & 18.7567 & -0.012468 & 0.035501 & -0.002132 \\ -0.052569 & -0.012468 & 0.0096831 & 6.0841\text{E-}06 & 0.0029395 \\ 0.061823 & 0.035501 & 6.0841\text{E-}06 & -0.0050423 & -0.0017709 \\ -1.5114\text{E-}06 & -0.002132 & 0.0029395 & -0.0017709 & -0.032403 \end{bmatrix}$$

$$\alpha = 21.7805 \quad (4.17)$$

Considering that the uncertain parameter $\delta(t)$ can vary independently from the state variable $x(t)$, I am looking for a region ε_α^* , in which the value of $V(x, \delta)$ is smaller than α for every possible values of $\delta(t) \in \mathcal{D}$, therefore, the region ε_α^* can be calculated as presented in equation (4.16).

3. Finally, $\delta = \delta(x_1)$ is known parameter, but it depends on the state variable x_1 . In this case, determining the domain of $\dot{\delta}$ is slightly more complicated, because \dot{x}_1 appears in the expansion of $\dot{\delta}$. Let $\delta = a + b \sin(\omega x_1)$. Fortunately, $\dot{x}_1 = -x_2$ easily implies that $\dot{\delta} = -b\omega x_2 \cos(\omega x_1)$. The maximum amplitude of $\dot{\delta}$ is $b\omega x_2^{(\max)}$, where the extremal value of x_2 can be computed from the polytope \mathcal{X} . It is important to consider that the sign of the cosine in the expression of $\dot{\delta}$ varies independently from the amplitude of $\dot{\delta}$, therefore, $x_2^{(\max)} = \max_{x \in \mathcal{X}} |x_2|$. Consequently, the value of $\dot{\delta}$ is an element of the interval $\check{\mathcal{D}} = [-\omega b x_2^{(\max)} \quad \omega b x_2^{(\max)}]$. In the numerical computations the parameters (a, b, ω) were given the values $(2, 1.5, 10)$. The area of the estimated DOA is $A = 3.5895u^2$. The generated Lyapunov function and its maximal invariant level set are:

$$P = \begin{bmatrix} 19.073 & -3.1506 & -0.018822 & 0.017114 & -0.00050213 \\ -3.1506 & 17.1091 & -0.015033 & 0.0549 & -0.0018608 \\ -0.018822 & -0.015033 & 0.00022283 & 1.5593\text{E-}05 & -0.0034762 \\ 0.017114 & 0.0549 & 1.5593\text{E-}05 & -0.024593 & 0.0042279 \\ -0.00050213 & -0.0018608 & -0.0034762 & 0.0042279 & 0.0031101 \end{bmatrix}$$

$$\alpha = 20.3254 \tag{4.18}$$

In comparison with the previous to cases, the values of the state variables determine the value of the uncertain parameter δ . Practically, the Lyapunov function depends only on the state vector x . Consequently, the maximal invariant region ε_α is calculated as the α -level set of the function $\hat{V}(x) = [V(x, \delta)]_{\delta=\delta(x)}$.

In all the presented cases, the polytope \mathcal{X} is evaluated gradually in an automated manner as described in Section 3.5. The initial polytope was chosen to be $\mathcal{X}^{(0)} = [-0.3, 0.3]^2$. The corners of the final polytopes in the three different cases are the following:

$$\vartheta(\mathcal{X}_1) : \begin{bmatrix} -1.3012 & -1.254 & -0.92327 & -0.30907 & 0.21064 & 0.63586 & 1.0217 & \dots \\ -0.093464 & -0.94709 & -1.4997 & -1.6628 & -1.3761 & -0.98564 & -0.51164 & \dots \\ \dots & 1.2996 & 1.2501 & 0.91934 & 0.30513 & -0.21458 & -0.64198 & -1.0284 & -1.3012 \\ \dots & 0.086228 & 0.94399 & 1.4907 & 1.6583 & 1.3748 & 0.98303 & 0.50474 & -0.093464 \end{bmatrix} \tag{4.19}$$

$$\vartheta(\mathcal{X}_2) : \begin{bmatrix} -1.1027 & -1.0586 & -0.80391 & -0.43838 & 0.1741 & 0.59969 & 0.90921 & \dots \\ 0.15356 & -0.41983 & -0.81969 & -1.0596 & -1.1088 & -0.92089 & -0.61639 & \dots \\ \dots & 1.1027 & 1.0586 & 0.80359 & 0.43702 & -0.1741 & -0.59969 & -0.90921 & -1.1027 \\ \dots & -0.15355 & 0.41986 & 0.81971 & 1.0596 & 1.1088 & 0.92134 & 0.61649 & 0.15356 \end{bmatrix} \tag{4.20}$$

$$\vartheta(\mathcal{X}_3) : \begin{bmatrix} -1.115 & -1.0286 & -0.72375 & -0.29341 & 0.25429 & 0.64551 & 0.95848 & \dots \\ -0.023927 & -0.55731 & -0.96418 & -1.1669 & -1.1178 & -0.88651 & -0.5051 & \dots \\ \dots & 1.115 & 1.03 & 0.72375 & 0.29341 & -0.25429 & -0.64551 & -0.95848 & -1.115 \\ \dots & 0.023403 & 0.5572 & 0.96671 & 1.1679 & 1.1172 & 0.8857 & 0.50502 & -0.023927 \end{bmatrix} \tag{4.21}$$

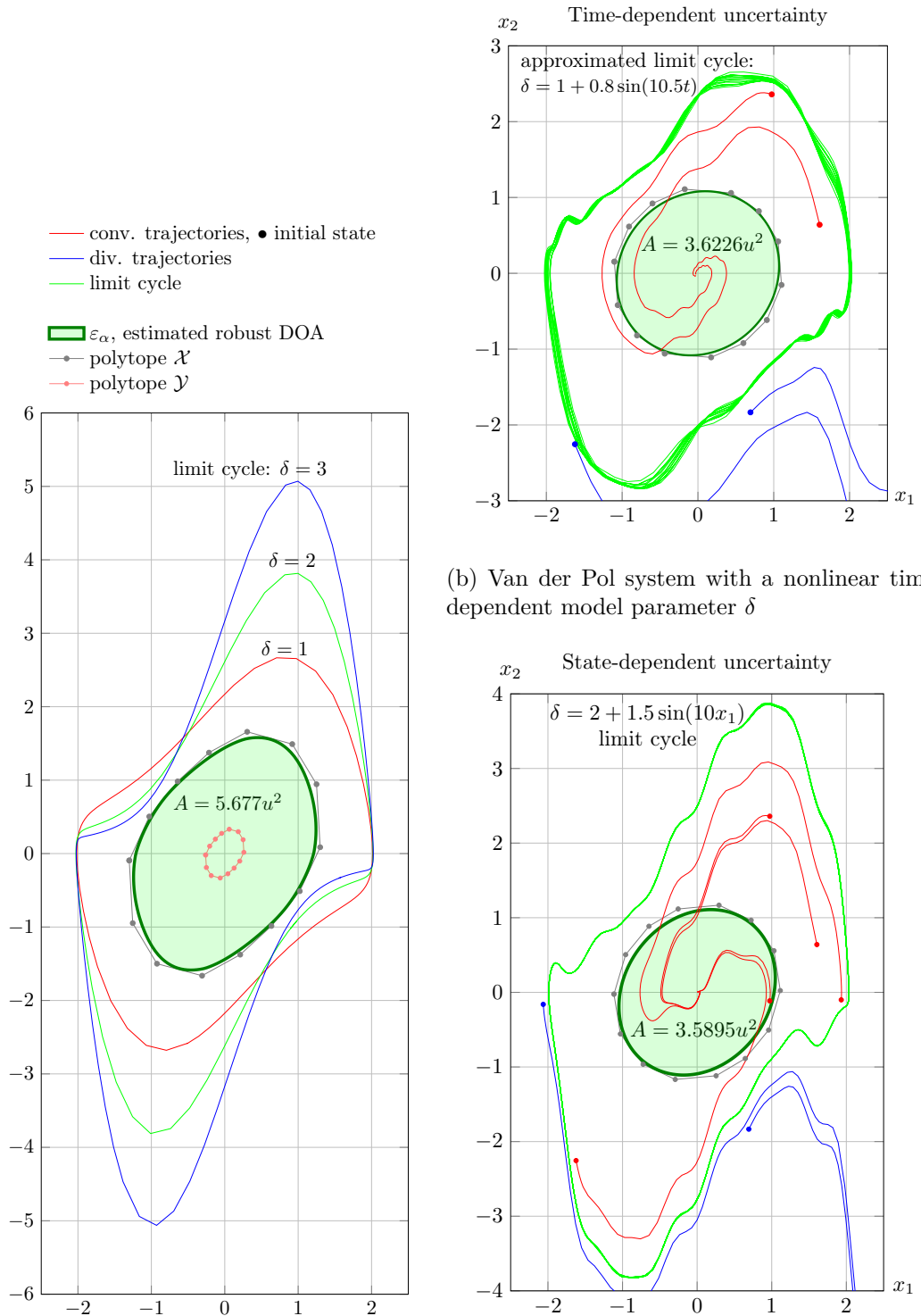


Figure 4.2: Time-inverted Van der Pol system with three different artificial uncertain model parameters

4.3 Mass-action kinetic systems

Mass-action kinetic (MAK) systems are used in chemistry and chemical engineering for the modeling of chemical reaction networks [26].

4.3.1 Time inverted Sel'kov model

The Sel'kov system [27]

$$\begin{aligned} \dot{x}_1 &= 1 - x_1 x_2^\gamma & \text{with } \gamma &= 2 \\ \dot{x}_2 &= \alpha x_2 (x_1 x_2^{\gamma-1} - 1) & \alpha &= 1.1 \end{aligned} \quad (4.22)$$

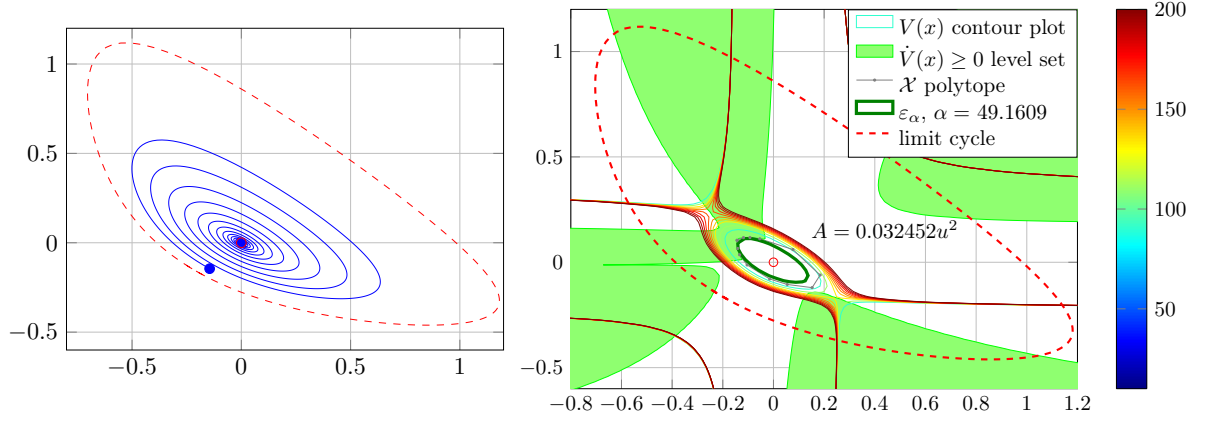
is a special case of MAK systems, which has an unstable steady state at $x_0 = [1, 1]$, and an attractive stable limit cycle. Substituting $\bar{x}(-t) + x_0$ into $x(t)$, I obtained a time inverted shifted system:

$$\begin{aligned} \dot{\bar{x}}_1 &= \bar{x}_1 + 2\bar{x}_2 + 2\bar{x}_1\bar{x}_2 + \bar{x}_1\bar{x}_2^2 + \bar{x}_2^2 \\ \dot{\bar{x}}_2 &= 1.1(-\bar{x}_1 - \bar{x}_2 - 2\bar{x}_1\bar{x}_2 - \bar{x}_1\bar{x}_2^2 - \bar{x}_2^2) \end{aligned} \quad (4.23)$$

which has an asymptotically stable steady state at the origin with an unstable limit cycle around it (Figure 4.3). However, the origin is “less attracting” than in case of the Van der Pol system in the sense that the Sel'kov system orbits around the origin several times before it converges to it (see blue trajectory in Figure 4.3a). Accordingly, estimating the DOA is more difficult in this case, and I cannot expect to obtain a large invariant level set.

The model matrices obtained using the consecutive transformations are:

$$\begin{aligned} A &= \begin{bmatrix} 1 & 2 \\ -1.1 & -1.1 \end{bmatrix} \\ B &= \begin{bmatrix} 2 & 1 & 1 \\ -2.2 & -1.1 & -1.1 \end{bmatrix} \\ \pi^T &= \begin{bmatrix} x_1 x_2 & x_1 x_2^2 & x_2^2 \end{bmatrix} \end{aligned} \quad \mathcal{N}_{\pi_b}(x) = \begin{bmatrix} 0 & 0 & 0 & 1 & -x_1 \\ 0 & 0 & x_2 & -1 & 0 \\ 0 & 0 & x_2 & 0 & -x_1 \\ 0 & x_1 & -1 & 0 & 0 \\ 0 & x_2 & 0 & 0 & -1 \\ x_2 & 0 & -1 & 0 & 0 \\ x_2 & -x_1 & 0 & 0 & 0 \end{bmatrix} \quad (4.24)$$



(a) Limit cycle (dashed red line), trajectory from a starting point inside the region of attraction (filled point). The blue trajectory indicates a slow convergence into the origin. (b) The level set ε (green line) is a bad approximation of the DOA due to the slow convergence of the system. The blue polygon constitutes the outer polytope \mathcal{X} .

Figure 4.3: Time inverted Sel'kov process

The value of P and α and the area of ε_α are:

$$P = \begin{bmatrix} 4847.7483 & 4412.1706 & -4.4108 & -189.8757 & 158.3735 \\ 4412.1706 & 8401.5745 & -541.1394 & -1542.4252 & -4626.3811 \\ -4.4108 & -541.1394 & 2329.3606 & 110556.3912 & 7641.0107 \\ -189.8757 & -1542.4252 & 110556.3912 & -966760.864 & 38803.7307 \\ 158.3735 & -4626.3811 & 7641.0107 & 38803.7307 & 38069.5409 \end{bmatrix} \quad (4.25)$$

$$\alpha = 49.1609, \quad A = 0.032452u^2 \quad (4.26)$$

The final polytope was defined manually by iteration:

$$\vartheta(\mathcal{X}) : \begin{bmatrix} -0.1436 & -0.1412 & -0.1339 & -0.1041 & -0.0149 & 0.0545 & \dots \\ 0.1042 & 0.0656 & 0.0355 & -0.0127 & -0.0792 & -0.1053 & \dots \\ \dots & 0.1526 & 0.1842 & 0.0767 & -0.054 & -0.0929 & -0.1183 & -0.1436 \\ \dots & -0.1204 & -0.0606 & 0.0605 & 0.1115 & 0.1174 & 0.1169 & 0.1042 \end{bmatrix} \quad (4.27)$$

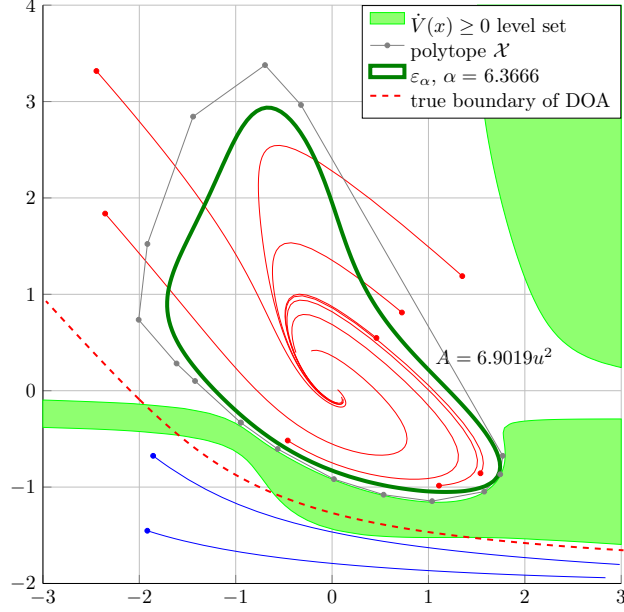


Figure 4.4: Minimal MAK system, trajectories from a few starting points (filled points). The blue trajectories tend to infinity while the red ones converge to the origin.

4.3.2 Minimal MAK system with an unbounded DOA

During my work I used a modified model presented by Wilhelm et.al. [28] with a specific parameter configuration:

$$\begin{aligned} \dot{x}_1 &= v_1 - k_2 x_1 x_2^2 \\ \dot{x}_2 &= k_2 x_1 x_2^2 - k_3 x_2 \end{aligned}, \quad \text{where} \quad \begin{aligned} v_1 &= 4 \\ k_2 &= 1 \\ k_3 &= 2 \end{aligned} \quad (4.28)$$

This model with these parameter values has an unbounded DOA and a stable steady state at $x_0^T = [x_1 \ x_2] = [\frac{v_1}{k_3} \ \frac{k_3^2}{k_2 v_1}] = [2 \ 1]$

In order to analyze the stability region of x_0 , I have translated the equilibrium point into the origin by substituting $\bar{x} + x_0$ into x obtaining the following:

$$\begin{aligned} \dot{\bar{x}}_1 &= -\frac{k_2 v_1^2}{k_3^2} \bar{x}_1 - 2 k_3 \bar{x}_2 - \frac{2 k_2 v_1}{k_3} \bar{x}_1 \bar{x}_2 - k_2 \bar{x}_1 \bar{x}_2^2 - \frac{k_3^2}{v_1} \bar{x}_2^2 \\ \dot{\bar{x}}_2 &= \frac{k_2 v_1^2}{k_3^2} \bar{x}_1 + k_3 \bar{x}_2 + \frac{2 k_2 v_1}{k_3} \bar{x}_1 \bar{x}_2 + k_2 \bar{x}_1 \bar{x}_2^2 + \frac{k_3^2}{v_1} \bar{x}_2^2 \end{aligned} \quad (4.29)$$

After substituting the numerical values into the parameters v_1, k_2, k_3 I got:

$$\begin{aligned} \dot{\bar{x}}_1 &= -4 \bar{x}_1 - 4 \bar{x}_2 - 4 \bar{x}_1 \bar{x}_2 - \bar{x}_1 \bar{x}_2^2 - \bar{x}_2^2 \\ \dot{\bar{x}}_2 &= 4 \bar{x}_1 + 2 \bar{x}_2 + 4 \bar{x}_1 \bar{x}_2 + \bar{x}_1 \bar{x}_2^2 + \bar{x}_2^2 \end{aligned} \quad (4.30)$$

Executing the consecutive model transformations, the model matrices are the following:

$$\begin{aligned}
 A &= \begin{bmatrix} -4 & -4 \\ 4 & 2 \end{bmatrix} \\
 B &= \begin{bmatrix} -4 & -1 & -1 \\ 4 & 1 & 1 \end{bmatrix} \\
 \pi^T &= \begin{bmatrix} x_1 x_2 & x_1 x_2^2 & x_2^2 \end{bmatrix} \\
 \mathcal{N}_{\pi_b}(x) &= \begin{bmatrix} 0 & 0 & 0 & 1 & -x_1 \\ 0 & 0 & x_2 & -1 & 0 \\ 0 & 0 & x_2 & 0 & -x_1 \\ 0 & x_1 & -1 & 0 & 0 \\ 0 & x_2 & 0 & 0 & -1 \\ x_2 & 0 & -1 & 0 & 0 \\ x_2 & -x_1 & 0 & 0 & 0 \end{bmatrix}
 \end{aligned} \tag{4.31}$$

The Lyapunov function and its maximal invariant level set are described by:

$$P = \begin{bmatrix} 4.3344 & 4.1886 & 1.709\text{E-}3 & 3.149\text{E-}5 & 1.0377\text{E-}4 \\ 4.1886 & 5.5407 & -0.47346 & -1.3918\text{E-}5 & -1.8757 \\ 1.709\text{E-}3 & -0.47346 & 0.43649 & 0.45061 & -0.17843 \\ 3.149\text{E-}5 & -1.3918\text{E-}5 & 0.45061 & 6.0537\text{E-}3 & 0.23054 \\ 1.0377\text{E-}4 & -1.8757 & -0.17843 & 0.23054 & 0.90654 \end{bmatrix} \tag{4.32}$$

$$\alpha = 6.3666, \quad A = 6.9019u^2 \tag{4.33}$$

The final polytope was defined manually by iteration:

$$\vartheta(\mathcal{X}) : \begin{bmatrix} -0.94797 & -0.5647 & 0.019036 & 0.5345 & 1.0376 & 1.5789 & 1.7445 & 1.7705 & \dots \\ -0.33122 & -0.605 & -0.91751 & -1.079 & -1.1459 & -1.0466 & -0.8672 & -0.67511 & \dots \\ \dots & -0.3227 & -0.6958 & -1.442 & -1.916 & -2.0067 & -1.6134 & -1.4218 & -0.94797 \\ \dots & 2.9647 & 3.3782 & 2.8437 & 1.5227 & 0.7361 & 0.2824 & 0.1008 & -0.33122 \end{bmatrix} \tag{4.34}$$

The results of the computations can be seen in Figure 4.4.

4.4 Third order rational system

In order to illustrate the performance of the algorithm, a third order rational system is taken from [1]:

$$\begin{aligned}\dot{x}_1 &= x_2 + \varepsilon_3 x_3 + \varepsilon_1 \zeta(x) \\ \dot{x}_2 &= -x_1 - x_2 + \varepsilon_2 x_1^2 \\ \dot{x}_3 &= \varepsilon_3(-2x_1 - 2x_3 - x_1^2)\end{aligned}\quad (4.35)$$

where

$$\zeta(x) = \frac{x_1}{x_2^2 + 1}, \quad x = \begin{bmatrix} x_1 \\ x_2 \\ x_3 \end{bmatrix}$$

$$\varepsilon_1 = \varepsilon_2 = \varepsilon_3 = \frac{1}{2}$$

This system has a locally asymptotically stable equilibrium point at the origin. This fact is implied by the negative eigenvalues of matrix A , which is in fact the Jacobian matrix of the system at the equilibrium. The model matrices A and B obtained for this system are the following:

$$A = \begin{bmatrix} 0.5 & 1 & 0.5 \\ -1 & -1 & 0 \\ -1 & 0 & -1 \end{bmatrix}\quad (4.36)$$

$$B = \begin{bmatrix} 0 & 0 & 0 & -0.5 & 0 & 0 \\ 0 & 0 & 0.5 & 0 & 0 & 0 \\ 0 & 0 & -0.5 & 0 & 0 & 0 \end{bmatrix}\quad (4.37)$$

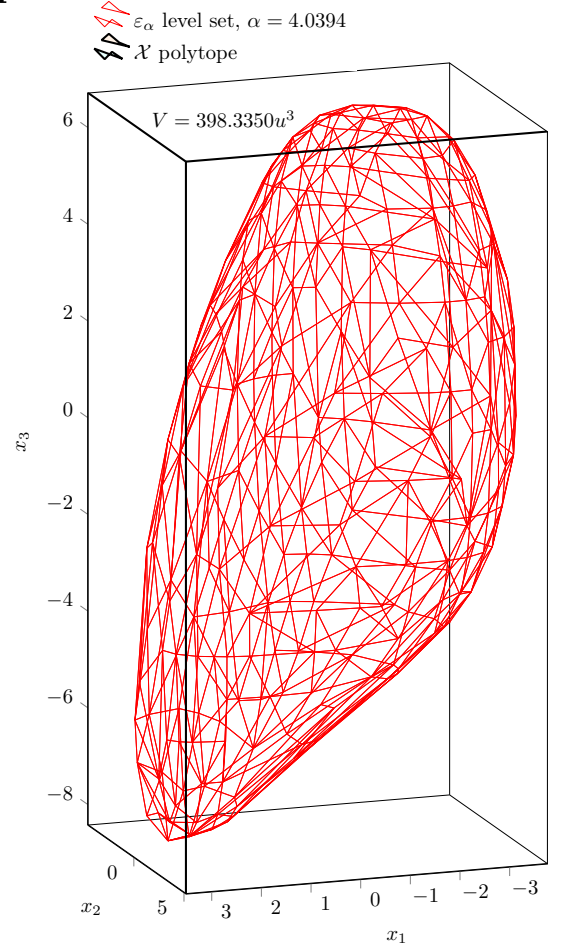


Figure 4.5: Estimated DOA of the third order rational system illustrated by the red polygon. The outer rectangular polygon constitutes the polytope \mathcal{X} .

The column vector π and the annihilator of π_b are:

$$\pi^T = \begin{bmatrix} x_1 x_2 \zeta(x) & x_1 \zeta(x) & x_1^2 & x_2^2 \zeta(x) & x_2 \zeta(x) & x_1 x_2 \end{bmatrix} \quad (4.38)$$

$$\mathcal{N}_{\pi_b}(x, \delta) = \begin{bmatrix} 0 & 0 & 0 & 0 & 0 & 0 & 1 & -x_2 & 0 \\ 0 & 0 & 0 & 0 & 0 & x_2 & 0 & 0 & -x_1 \\ 0 & 0 & 0 & 0 & x_2 & 0 & 0 & -x_1 & 0 \\ 0 & 0 & 0 & 1 & 0 & 0 & 0 & -x_1 & 0 \\ 0 & 0 & 0 & 1 & -x_2 & 0 & 0 & 0 & 0 \\ 0 & 0 & 0 & x_2 & 0 & 0 & -x_1 & 0 & 0 \\ 0 & x_1 & 0 & 0 & 0 & 0 & 0 & 0 & -1 \\ 0 & x_3 & -x_2 & 0 & 0 & 0 & 0 & 0 & 0 \\ x_1 & 0 & 0 & 0 & -1 & 0 & -x_1 & 0 & 0 \\ x_1 & 0 & 0 & 0 & 0 & -1 & 0 & 0 & 0 \\ x_2 & 0 & 0 & 0 & 0 & 0 & 0 & 0 & -1 \\ x_2 & 0 & 0 & 0 & 0 & 0 & -x_2 & -1 & 0 \\ x_2 & -x_1 & 0 & 0 & 0 & 0 & 0 & 0 & 0 \\ x_3 & 0 & -x_1 & 0 & 0 & 0 & 0 & 0 & 0 \end{bmatrix} \quad (4.39)$$

The maximal invariant level set of $V(x) = \pi_b^T P \pi_b$, and the generated matrix P are:

$$P = \begin{bmatrix} 0.24682 & 0.048679 & 0.11214 & 0.042366 & -14.9084 & 14.9247 & -0.050515 & 12.3269 & -12.2731 \\ 0.048679 & 0.2128 & 0.031464 & 0.021364 & 0.10189 & -0.15608 & -0.047148 & 0.060929 & 0.021878 \\ 0.11214 & 0.031464 & 0.11504 & -0.0067033 & 0.00080533 & 0.0178 & -0.0095644 & -0.0020643 & 0.0040921 \\ 0.042366 & 0.021364 & -0.0067033 & 0.01445 & -0.00141 & -0.0030255 & -3.9744 & 3.9999 & -4.0343 \\ -14.9084 & 0.10189 & 0.00080533 & -0.00141 & 0.0031407 & 0.0025979 & -4.0152 & -3.9773 & 5.268 \\ 14.9247 & -0.15608 & 0.0178 & -0.0030255 & 0.0025979 & 0.011247 & -10.8675 & -1.3232 & -0.0065652 \\ -0.050515 & -0.047148 & -0.0095644 & -3.9744 & -4.0152 & -10.8675 & 56.6889 & -0.023007 & 12.3672 \\ 12.3269 & 0.060929 & -0.0020643 & 3.9999 & -3.9773 & -1.3232 & -0.023007 & 56.4424 & -28.2011 \\ -12.2731 & 0.021878 & 0.0040921 & -4.0343 & 5.268 & -0.0065652 & 12.3672 & -28.2011 & 0.014463 \end{bmatrix}$$

$$\varepsilon_\alpha = \{x \in \mathcal{X} \mid V(x) = \alpha = 4.0394\} \quad (4.40)$$

The volume of the estimated DOA for the system in [1] is $32.022u^3$. My improved automated algorithm by applying the LFT generates an invariant level set of $398.3350u^3$. The possible cause of this difference can be the increased numerical stability obtained by the dimension reduction of the problem by considering fewer entries in π and eliminating the repetitive (redundant) rows from the annihilator matrices.

The polytope \mathcal{X} was generated automatically, and it was bound to be a rectangular region, which results in a smaller number of facets being considered in the optimization task, furthermore, this regularity assumption makes easier to approximate iteratively the most appropriate rectangular \mathcal{X} . The estimated DOA is shown in Figure 4.5. The final polytope was: $\mathcal{X} = [-3.7710, 3.5195] \times [-4.6077, 5.1943] \times [-8.4274, 6.7204]$.

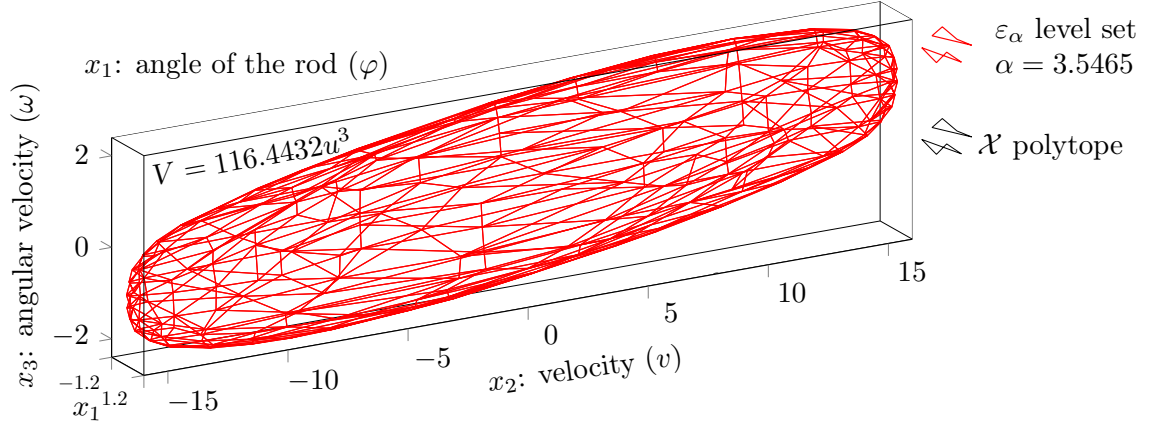


Figure 4.6: Estimated DOA of the inverted pendulum is illustrated by the red polygon. The outer polytope was chosen manually as $\mathcal{X} = [-1.2, 1.2] \times [-16, 16] \times [-2.4, 2.4]$.

4.5 Stability of a controlled inverted pendulum

Especially in robotics, there appear nonlinear mechanical models containing trigonometric functions, for which the stability analysis is often a challenging task. The inverted pendulum is a classical bench-mark example for this class of nonlinearities. In Section 4.2, I have already presented a nonlinear system (uncertain Van der Pol) featuring a sinusoid nonlinearity, which was wrapped into a state-dependent uncertain parameter. However, in case of the pendulum, important characteristic features disappear from the dynamics if I try this approach. Instead, I used Taylor approximation of the trigonometric nonlinearities, and a Lyapunov function $V(x)$ is computed using the simplified rational model. Then, I check the negativity of the time derivative of the obtained Lyapunov function on the whole \mathcal{X} , and $\dot{V}(x)$ is computed by substituting the original (trigonometric) dynamics into \dot{x} .

The inverted pendulum system, can be described by the following 4th order differential equation:

$$\frac{d\hat{x}}{dt} = f(\hat{x}) + g(\hat{x})u, \quad \text{where } \hat{x}^T = [r \ \varphi \ v \ \omega] \quad (4.41)$$

$$f(\hat{x}) = \begin{bmatrix} v \\ \omega \\ \frac{1}{q(\varphi)}(-4ml\omega^2 \sin(\varphi) + 1.5mg \sin(2\varphi)) \\ \frac{1}{lq(\varphi)}(-1.5ml\omega^2 \sin(2\varphi) + 3g(m+M) \sin(\varphi)) \end{bmatrix} \quad (4.42)$$

$$g(\hat{x}) = \frac{1}{lq(\varphi)} \begin{bmatrix} 0 \\ 0 \\ 4l \\ 3 \cos(\varphi) \end{bmatrix}, \quad \text{where } q(\varphi) = 4(m+M) - 3m(\cos \varphi)^2 \quad (4.43)$$

The variables and parameters of the system are listed in the following table.

r	linear position of the chart		[m]
φ	angle of the rod with the vertical		[rad]
v	linear velocity of the chart		[m/s]
ω	angular velocity of the rod		[rad/s]
l	length of the rod	1	[m]
m	mass of the rod	0.5	[kg]
M	mass of the chart	1	[kg]
g	gravitational accelerations	9.8	[m/s ²]

Since the linear position of the chart r does not appear on the right hand side of equation (4.41), the dynamics of the system does not depend on r . In other words, the linear position r has no effect on the system's dynamics, therefore, the first equation ($\dot{r} = v$) can be omitted from the stability analysis as it is often done in literature. Let the state vector of the reduced system be $x^T = [x_1 \ x_2 \ x_3]$, where $x_1 = \varphi$, $x_2 = v$ and $x_3 = \omega$. This system has an unstable equilibrium point at the origin, which can be locally stabilized using a static state feedback $u = -Kx$, where the row vector $K \in \mathbb{R}^3$ is the feedback gain. The 3rd order model is of the form $\dot{x} = h(x)$, where

$$h(x) = \begin{bmatrix} x_3 \\ \frac{1}{q(x_1)} (-4mlx_3^2 \sin(x_1) + 1.5mg \sin(2x_1) - 4Kx) \\ \frac{1}{lq(x_1)} (-1.5mlx_3^2 \sin(2x_1) + 3g(m+M) \sin(x_1) - 3 \cos(x_1)Kx) \end{bmatrix} \quad (4.44)$$

As the LFT cannot handle trigonometric nonlinearities, these functions are approximated around the equilibrium point by (at most) a 2nd order Taylor polynomial:

$$\begin{aligned} \sin(x_1) &\simeq x_1 \\ \cos(x_1) &\simeq 1 - 0.5x_1^2 \\ \cos(x_1)^2 &\simeq 1 - x_1^2 \end{aligned} \quad \zeta(x) := \frac{1}{3mx_1^2 + (m+4M)} \simeq \frac{1}{q(x_1)} \quad (4.45)$$

The resulting rational nonlinear system will be $\dot{x} = \tilde{h}(x)$, where

$$\tilde{h}(x) = \frac{1}{l} \begin{bmatrix} lx_3 \\ \zeta(x) (-4ml^2x_1x_3^2 + 3mglx_1 - 4lKx) \\ \zeta(x) (-3mlx_1x_3^2 + 3g(m+M)x_1 - 3(1-x_1^2)Kx) \end{bmatrix} \quad (4.46)$$

In the numerical computations, the feedback gain K has the value [36 -1 12], which is the rounded value of an optimal feedback gain generated by a linear quadratic regulator (LQR) design. The system with this rounded feedback gain is still locally asymptotically stable. Substituting the numerical values into the parameters l , m , M , g , the model

$\dot{x} = \tilde{h}(x)$ can be transformed into the representation (2.11):

$$\begin{aligned}
A &= \begin{bmatrix} 0 & 0 & 1 \\ -28.7333 & 0.88889 & -10.6667 \\ -14.2 & 0.66667 & -8 \end{bmatrix}, \quad B = \begin{bmatrix} 0 & 0 & 0 & 0 & 0 & 0 & 0 \\ 9.5778 & 0 & -0.2963 & 0 & 3.5556 & 0 & -0.44444 \\ 16.7333 & 0 & -0.55556 & 0 & 6.6667 & 0 & -0.33333 \end{bmatrix} \\
\pi &= \frac{3}{x_1^2+3} \begin{bmatrix} x_1^3 \\ x_1^2 \\ x_1^2 x_2 \\ x_1 x_2 \\ x_1^2 x_3 \\ x_1 x_3 \\ x_1 x_3^2 \end{bmatrix} \quad \mathcal{N}_{\pi_b}(x) = \begin{bmatrix} 0 & 0 & 0 & 0 & 0 & 0 & 0 & 0 & x_3 & -1 \\ 0 & 0 & 0 & 0 & 0 & 0 & 0 & 0 & 1 & -x_1 & 0 \\ 0 & 0 & 0 & 0 & 0 & 0 & 0 & 0 & x_3 & 0 & -x_1 \\ 0 & 0 & 0 & 0 & 0 & 0 & x_3 & 0 & 0 & -x_2 & 0 \\ 0 & 0 & 0 & 0 & 0 & 1 & -x_1 & 0 & 0 & 0 & 0 \\ 0 & 0 & 0 & 0 & 0 & x_3 & 0 & 0 & -x_2 & 0 & 0 \\ 0 & 0 & 0 & 0 & x_2 & -1 & 0 & 0 & 0 & 0 & 0 \\ 0 & 0 & 0 & 0 & x_2 & 0 & -x_1 & 0 & 0 & 0 & 0 \\ 0 & 0 & 0 & 0 & x_3 & 0 & 0 & -1 & 0 & 0 & 0 \\ 0 & 0 & 0 & 0 & x_3 & 0 & 0 & 0 & 0 & -x_1 & 0 \\ 0 & 0 & 0 & 1 & -x_1 & -\frac{1}{36} & \frac{x_1}{36} & \frac{1}{3} & -\frac{x_1}{3} & 0 & 0 \\ 0 & 0 & 0 & 1 & -x_1 & 0 & 0 & 0 & 0 & 0 & 0 \\ 0 & 0 & 0 & x_2 & 0 & -x_1 & 0 & 0 & 0 & 0 & 0 \\ 0 & 0 & 0 & x_3 & 0 & 0 & 0 & -x_1 & 0 & 0 & 0 \\ 0 & 0 & x_1 & 0 & 0 & 0 & 0 & -\frac{x_1}{3} & -1 & 0 & 0 \\ 0 & x_1 & 0 & 0 & 0 & -\frac{x_1}{3} & -1 & 0 & 0 & 0 & 0 \\ 0 & x_3 & -x_2 & 0 & 0 & 0 & 0 & 0 & 0 & 0 & 0 \\ x_1 & 0 & 0 & -\frac{x_1}{3} & -1 & 0 & 0 & 0 & 0 & 0 & 0 \\ x_2 & 0 & 0 & -\frac{x_2}{3} & 0 & 0 & -1 & 0 & 0 & 0 & 0 \\ x_2 & -x_1 & 0 & 0 & 0 & 0 & 0 & 0 & 0 & 0 & 0 \\ x_3 & 0 & 0 & -\frac{x_3}{3} & 0 & 0 & 0 & 0 & -1 & 0 & 0 \\ x_3 & 0 & -x_1 & 0 & 0 & 0 & 0 & 0 & 0 & 0 & 0 \end{bmatrix} \quad (4.47)
\end{aligned}$$

The matrix P from the Lyapunov function, the maximal invariant level set and its volume are:

$$\begin{aligned}
P &= \begin{bmatrix} 3.7519 & -0.092361 & 0.44941 & -1537.3922 & -1.9857\text{E-}08 & 3723.7945 & 0.00090873 & -1517.9758 & -0.0044609 & -3207.8085 \\ -0.092361 & 0.019392 & -0.069085 & -3595.1177 & -0.00090873 & 0.043468 & -1.3016\text{E-}10 & -12.5226 & 5.0049 & 0.0412 \\ 0.44941 & -0.069085 & 0.86706 & 9.124 & 0.004461 & -0.04595 & -5.0049 & 3446.765 & -1.3857\text{E-}09 & -0.13625 \\ -1537.3922 & -3595.1177 & 9.124 & 1020.752 & 1.0702\text{E-}08 & -42.8946 & 16.2659 & 502.2325 & -0.0032803 & 1027.9664 \\ -1.9857\text{E-}08 & -0.00090873 & 0.004461 & 1.0702\text{E-}08 & 3081.1585 & -16.2659 & -128.4693 & 0.0032802 & 1508.4604 & -0.00036152 \\ 3723.7945 & 0.043468 & -0.04595 & -42.8946 & -16.2659 & -0.031519 & 1.0843\text{E-}10 & 4.0599 & -4754.3435 & 0.0077353 \\ 0.00090873 & -1.3016\text{E-}10 & -5.0049 & 16.2659 & -128.4693 & 1.0843\text{E-}10 & -0.11092 & 4754.3435 & 12.7507 & -1.8194\text{E-}09 \\ -1517.9758 & -12.5226 & 3446.765 & 502.2325 & 0.0032802 & 4.0599 & 4754.3435 & -2213.8946 & 0.00036151 & 0.1324 \\ -0.0044609 & 5.0049 & -1.3857\text{E-}09 & -0.0032803 & 1508.4604 & -4754.3435 & 12.7507 & 0.00036151 & -478.3034 & 1.9762\text{E-}08 \\ -3207.8085 & 0.0412 & -0.13625 & 1027.9664 & -0.00036152 & 0.0077353 & -1.8194\text{E-}09 & 0.1324 & 1.9762\text{E-}08 & 0.010434 \end{bmatrix} \\
\varepsilon_\alpha &= \{x \in \mathcal{X} \mid V(x) = \alpha = 3.5465\}, \quad V = 116.4431u^3 \quad (4.48)
\end{aligned}$$

The estimated DOA is shown in Figure 4.6. The polytope \mathcal{X} was chosen manually: $\mathcal{X} = [-1.2, 1.2] \times [-16, 16] \times [-2.4, 2.4]$.

Table 4.1: Variables and parameters of the fermentation process

X	Biomass concentration		$[g/l]$
S	Substrate concentration		$[g/l]$
F	Feed flow rate		$[l/h]$
V	Volume	4	$[l]$
S_F	Substrate feed concentration	10	$[g/l]$
Y	Yield coefficient	0.5	
μ_{max}	maximal growth rate	1	$[l/h]$
K_1	Saturation parameter	0.03	$[g/l]$
K_2	Inhibition parameter	0.5	$[l/g]$
Steady-state operating point:			
X_0	equilibrium point of X	4.8907	$[g/l]$
S_0	equilibrium point of S	0.2187	$[g/l]$
F_0	Inlet feed flow rate	3.2089	$[l/h]$

4.6 A continuous fermentation process

It is known that bioreactors often show strongly nonlinear dynamical behaviour and their efficient control is a challenging task [29].

In this section, I present an isothermal nonlinear continuous fermentation process model taken from [2] with constant volume V and constant physico-chemical properties. The dynamics of the process is given by the state-space model

$$\frac{dX}{dt} = \mu(S)X - \frac{XF}{V} \quad (\text{biomass component mass balance}) \quad (4.49)$$

$$\frac{dS}{dt} = \frac{\mu(S)X}{Y} + \frac{(S_F - S)F}{V} \quad (\text{substrate component mass balance}) \quad (4.50)$$

$$\mu(S) = \mu_{max} \frac{S}{K_2 S^2 + S + K_1} \quad (\text{growth rate function}) \quad (4.51)$$

The variables and parameters of the model together with their units and values are given in Table 4.1. The above model can be easily written in standard input-affine form with the centered state vector

$$x = [x_1 \quad x_2]^T = [S - S_0 \quad X - X_0]^T \quad (4.52)$$

consisting of the centered biomass and substrate concentrations. The centered input flow rate is chosen as a manipulate input variable as follows: $u = F - F_0$. The centered model is: $\dot{x} = f(x) + g(x)u$

$$f(x) = \begin{bmatrix} (x_1 + X_0) \cdot \mu(x_2 + S_0) & -\frac{(x_1 + X_0)F_0}{V} \\ -\frac{(x_1 + X_0) \cdot \mu(x_2 + S_0)}{Y} & +\frac{(S_F - (x_2 + S_0))F_0}{V} \end{bmatrix} \quad (4.53)$$

$$g(x) = -\frac{1}{V} \begin{bmatrix} x_1 + X_0 \\ x_2 + S_0 - S_F \end{bmatrix} \quad (4.54)$$

The origin of the coordinates system is an equilibrium point if

$$f(0) = \begin{bmatrix} X_0 \cdot \mu(S_0) - X_0 F_0 / V \\ -X_0 \cdot \mu(S_0) / Y + (S_F - S_0) F_0 / V \end{bmatrix} = 0, \quad (4.55)$$

meaning that $F_0 = V\mu(S_0)$ and $X_0 = (S_F - S_0)Y$. The coordinate S_0 of steady state operating point of the system is computed so that the biomass production $X_0 F_0$ is maximal:

$$S_0 = \arg \max_{S_0 > 0} (S_F - S_0)\mu(S_0) = \frac{-K_1 + \sqrt{K_1^2 + S_F^2 K_1 K_2 + S_F K_1}}{K_2 S_F + 1} \quad (4.56)$$

The computational steps of the previous statement can be seen in the sequel. Firstly, the expression of $X_0 S_0$ is transformed to a simplified form:

$$\begin{aligned} X_0 F_0 &= VY\mu(S_0)(S_F - S_0) = \mu_{max} VY \frac{-S_0^2 + S_F S_0}{K_2 S_0^2 + S_0 + K_1} \\ &= \frac{\mu_{max} VY}{K_2} \frac{-K_2 S_0^2 + K_2 S_F S_0}{K_2 S_0^2 + S_0 + K_1} \\ &= \frac{\mu_{max} VY}{K_2} \left(-1 + \frac{(K_2 S_F + 1)S_0 + K_1}{K_2 S_0^2 + S_0 + K_1} \right) \end{aligned} \quad (4.57)$$

In order to obtain the maximal value of the above expression, its derivative is computed with respect to S_0 .

$$\begin{aligned} \max_{S_0} : \frac{d}{dS_0} X_0(S_0)F_0(S_0) &= 0 \\ \Leftrightarrow \frac{d}{dS_0} \frac{(K_2 S_F + 1)S_0 + K_1}{K_2 S_0^2 + S_0 + K_1} &= 0 \\ \Leftrightarrow \frac{(K_2 S_F + 1)(K_2 S_0^2 + S_0 + K_1) - (2K_2 S_0 + 1)((K_2 S_F + 1)S_0 + K_1)}{(K_2 S_0^2 + S_0 + K_1)^2} &= 0 \\ \Leftrightarrow (K_2 S_F + 1)S_0^2 + 2K_1 S_0 - S_F K_1 &= 0 \end{aligned} \quad (4.58)$$

Finally, the optimal value of S_0 can be derived. The numerical operating point values are given in Table 4.1.

In the following, I present the computational results of the method. Firstly, the procedure is applied to the open-loop system, then the effect of a negative substrate feedback is analyzed.

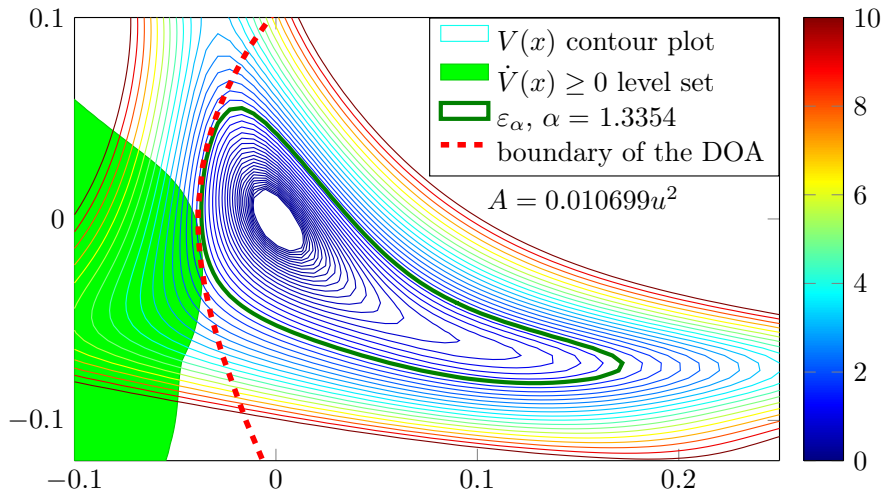
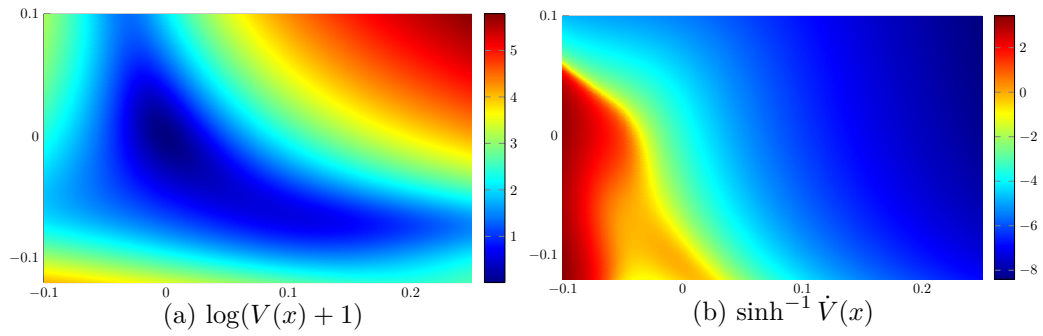


Figure 4.7: Lyapunov function and its derivative (OLS, $k = 0$)

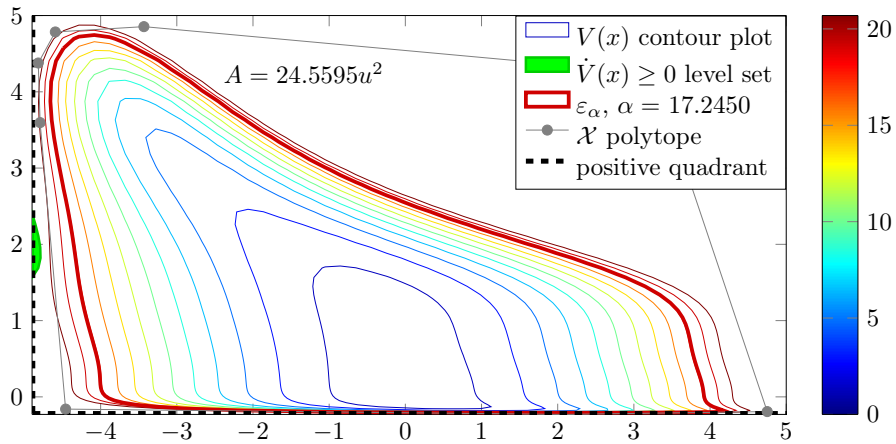
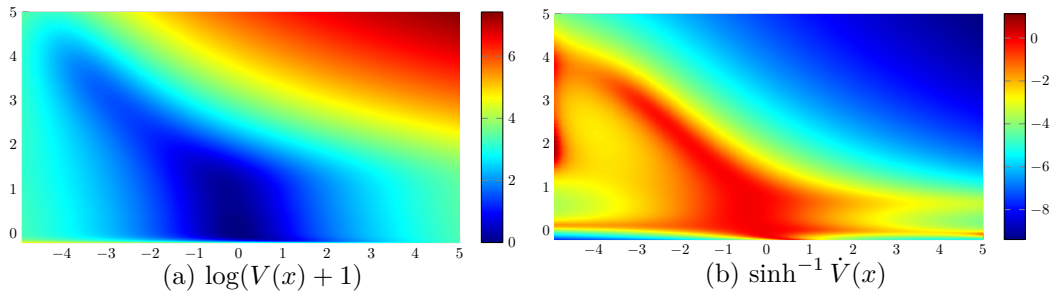


Figure 4.8: Lyapunov function and its derivative (CLS, $k = -0.8$)

4.6.1 Open-loop system (OLS)

If the centered input flow rate $u = 0$, the model can be transformed into the following nonlinear state-space model:

$$\begin{aligned} \dot{x} &= f(x) = A(x)x, \quad \text{where} \\ A(x) &= \begin{bmatrix} -\frac{F_0(c_2x_2^2 + c_1x_2)}{q(x_2)V} & \frac{\mu_{max}V(x_1 + X_0) - X_0F_0(c_2x_2 + c_1)}{q(x_2)V} \\ -\frac{\mu_{max}S_0}{q(x_2)Y} & -\frac{F_0}{V} - \frac{\mu_{max}(x_1 + X_0)}{q(x_2)Y} - \frac{F_0(S_0 - S_F)(c_2x_2 + c_1)}{q(x_2)V} \end{bmatrix} \\ q(x_2) &= c_2x_2^2 + c_1x_2 + c_0 \quad c_1 = 2K_2S_0 + 1 \\ c_0 &= K_2S_0^2 + S_0 + K_1 \quad c_2 = K_2 \end{aligned} \quad (4.59)$$

The model matrices for this system are

$$\begin{aligned} A &= \begin{bmatrix} 0 & 0.40111 \\ -1.6045 & -1.6045 \end{bmatrix}, \quad B = \begin{bmatrix} 0.082016 & -1.4716 & -0.7358 & -8.9905 \\ -0.16403 & 2.9432 & 1.4716 & 17.981 \end{bmatrix} \\ \pi &= [x_1x_2 \quad x_1x_2^2 \quad x_2^3 \quad x_2^2]^T \cdot \zeta(x_2), \quad \text{where } \zeta(x_2) \simeq (3.6688q(x_2))^{-1} \end{aligned} \quad (4.60)$$

The approximated value of $\mathcal{N}_{\pi_b}(x)$ with 4 decimal digit accuracy is:

$$\mathcal{N}_{\pi_b}(x) = \begin{bmatrix} 0 & 0 & 0 & 0 & 1 & -x_2 \\ 0 & 0 & 0 & 1 & 0 & -x_1 \\ 0 & 0 & 0 & x_2 & -x_1 & 0 \\ 0 & 0 & x_2 & -1 & 0 & 0 \\ 0 & 0 & x_2 & 0 & 0 & -x_1 \\ 0 & -0.2463x_2 & 0 & 0 & 0.4517x_2 + 0.101 & x_2 + 0.2463 \\ 0 & -0.2237x_1 & 0.2237 & 0 & 0.4103x_1 & x_1 \\ 0 & -0.2237x_2 & 0 & 0 & 0.4103x_2 & x_2 + 0.2237 \\ x_2 & -x_1 & 0 & 0 & 0 & 0 \\ -0.2463x_2 & 0 & x_2 + 0.2463 & 0.4517x_2 + 0.101 & 0 & 0 \\ -0.2237x_2 & 0 & x_2 + 0.2237 & 0.4103x_2 & 0 & 0 \end{bmatrix} \quad (4.61)$$

The generated P , α and the area of the estimate are:

$$\begin{aligned} P &= \begin{bmatrix} 971.2401 & 450.6579 & 11177.6448 & 243310.7436 & 6332.5198 & -14173.4478 \\ 450.6579 & 637.0046 & 20799.7569 & 87571.9883 & -13185.8278 & 1712.5523 \\ 11177.6448 & 20799.7569 & -265074.8729 & -488241.4065 & 43817.9314 & -38256.3894 \\ 243310.7436 & 87571.9883 & -488241.4065 & -361262.1183 & -14259.2742 & -277713.8548 \\ 6332.5198 & -13185.8278 & 43817.9314 & -14259.2742 & -96549.5592 & -134720.6252 \\ -14173.4478 & 1712.5523 & -38256.3894 & -277713.8548 & -134720.6252 & 22741.6173 \end{bmatrix} \\ \alpha &= 1.3354, \quad A = 0.010699u^2 \end{aligned} \quad (4.62)$$

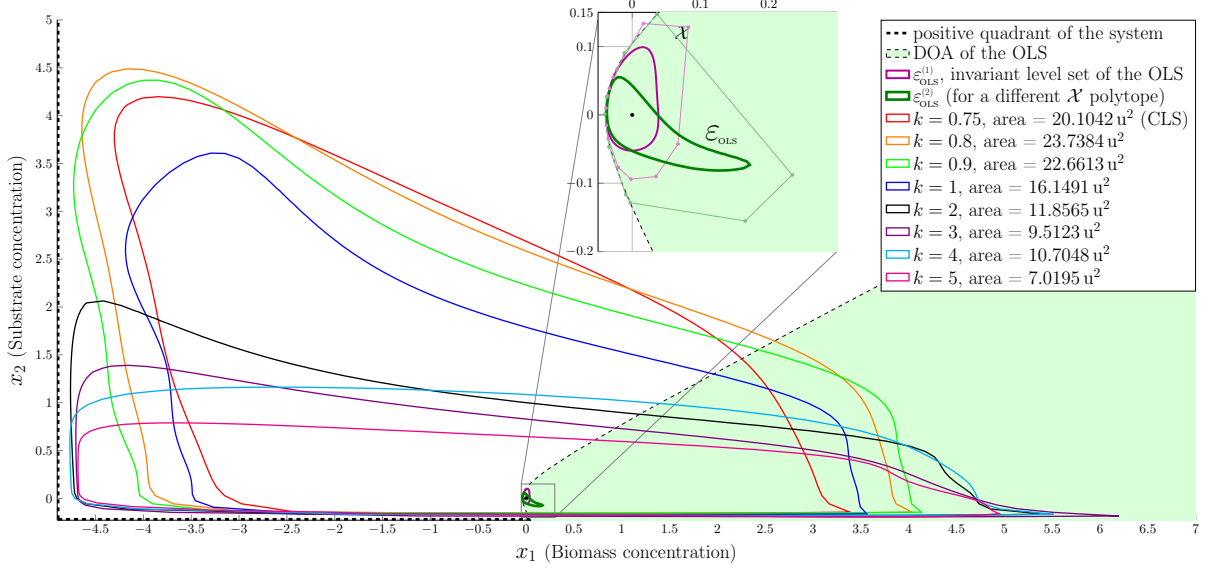


Figure 4.9: Green area: domain of attraction of the continuous fermentation process without feedback. The final invariant level set for the open-loop system (OLS) is shown in the magnified plot (magenta and green, for two different polytopes \mathcal{X}). The final invariant level sets for the closed loop system (CLS) are shown in different colors according to the different feedback gains k .

4.6.2 Effect of linear substrate feedback

Let us define the centered input flow rate as $u = -kx_2$, where $k > 0$ is the feedback gain. From (4.53,4.54), the equation of the closed-loop system can be transformed into the following form:

$$\dot{x} = \mathfrak{A}(x)x, \quad \text{where} \quad \mathfrak{A}(x) = \begin{bmatrix} \mathfrak{A}_{11}(x) & \mathfrak{A}_{12}(x) \\ \mathfrak{A}_{21}(x) & \mathfrak{A}_{22}(x) \end{bmatrix}$$

$$\mathfrak{A}_{11}(x) = -\frac{F_0(c_2x_2^2 + c_1x_2)}{r(x_2)V} - \frac{kx_2}{V}$$

$$\mathfrak{A}_{12}(x) = \frac{\mu_{max}V(x_1 + X_0) - X_0F_0(c_2x_2 + c_1)}{r(x_2)V} - \frac{kX_0}{V}$$

$$\mathfrak{A}_{21}(x) = -\frac{\mu_{max}S_0}{r(x_2)Y}$$

$$\mathfrak{A}_{22}(x) = \frac{F_0(S_F - S_0)(c_2x_2 + c_1)}{r(x_2)V} - \frac{\mu_{max}(x_1 + X_0)}{r(x_2)Y} - \frac{k(x_2 + S_0 - S_F) + F_0}{V}$$
(4.63)

After the necessary transformations and using $k = 0.8$ as a feedback gain, the rounded numerical values of model matrices with 4 decimal digit accuracy are

$$\begin{aligned}
A &= \begin{bmatrix} 0 & 1.3792 \\ -1.6045 & -3.5607 \end{bmatrix}, \quad B = \begin{bmatrix} 0.082016 & 0.2 & -1.4716 & -0.7358 & -8.9905 & 0 \\ -0.16403 & 0 & 2.9432 & 1.4716 & 17.981 & 0.2 \end{bmatrix} \\
\pi^T &= \left[(x_1 x_2) \zeta(x) \quad x_1 x_2 \quad (x_1 x_2^2) \zeta(x) \quad x_2^3 \zeta(x) \quad x_2^2 \zeta(x) \quad x_2^2 \right], \quad \zeta(x) \simeq (3.6688 q(x_2))^{-1} \\
\mathcal{N}_{\pi_6}(x, \delta) &= \begin{bmatrix} 0 & 0 & 0 & 0 & 0 & 1 & -x_2 & 0 \\ 0 & 0 & 0 & 0 & 1 & 0 & -x_1 & 0 \\ 0 & 0 & 0 & 0 & x_2 & -x_1 & 0 & 0 \\ 0 & 0 & 0 & x_2 & 0 & 0 & 0 & -x_1 \\ 0 & 0 & x_2 & 0 & -1 & 0 & 0 & 0 \\ 0 & 0 & x_2 & 0 & 0 & 0 & -x_1 & 0 \\ 0 & x_1 & 0 & -1 & 0 & 0 & 0 & 0 \\ 0 & x_2 & 0 & 0 & 0 & 0 & 0 & -1 \\ 0 & -0.2463x_2 & 0 & 0 & 0 & 0.4517x_2 + 0.101 & x_2 + 0.2463 & 0 \\ 0 & -0.2237x_1 & 0.2237 & 0 & 0 & 0.4103x_1 & x_1 & 0 \\ 0 & -0.2237x_2 & 0 & 0 & 0 & 0.4103x_2 & x_2 + 0.2237 & 0 \\ x_2 & 0 & 0 & -1 & 0 & 0 & 0 & 0 \\ x_2 & -x_1 & 0 & 0 & 0 & 0 & 0 & 0 \\ -0.2463x_2 & 0 & x_2 + 0.2463 & 0 & 0.4517x_2 + 0.101 & 0 & 0 & 0 \\ -0.2237x_2 & 0 & x_2 + 0.2237 & 0 & 0.4103x_2 & 0 & 0 & 0 \end{bmatrix}
\end{aligned} \tag{4.64}$$

The generated P , α and the area of the estimate are:

$$\begin{aligned}
P &= \begin{bmatrix} 1.1199 & 0.92033 & -30.625 & 30.4466 & -124.0099 & 135.835 & 17.7229 & -6.9136 \\ 0.92033 & 2.0768 & -107.4816 & 88.8882 & -484.882 & 98.0527 & -5.2247 & -12.5877 \\ -30.625 & -107.4816 & -33.3373 & 4.1097 & -67.6147 & 534.8658 & 48.412 & -21.4304 \\ 30.4466 & 88.8882 & 4.1097 & 2.1802 & -67.8471 & -387.9268 & -31.6243 & 0.78088 \\ -124.0099 & -484.882 & -67.6147 & -67.8471 & -7.4534 & -23.2976 & -348.0484 & 241.5972 \\ 135.835 & 98.0527 & 534.8658 & -387.9268 & -23.2976 & -215.8171 & -279.9563 & 23.7192 \\ 17.7229 & -5.2247 & 48.412 & -31.6243 & -348.0484 & -279.9563 & 87.3201 & 13.5614 \\ -6.9136 & -12.5877 & -21.4304 & 0.78088 & 241.5972 & 23.7192 & 13.5614 & 0.61819 \end{bmatrix} \\
\alpha &= 17.2450, \quad A = 24.5595u^2
\end{aligned} \tag{4.65}$$

The plot of the Lyapunov function and its time derivative is illustrated in Figure 4.8. I have measured the area of the estimated DOA using different feedback gains. The results of the computations can be seen in Figure 4.9 alongside the estimated DOA of the open-loop system. Apparently, the closed-loop system features a much larger invariant level set than the open-loop system. Thus, it is clearly shown that a simple linear substrate feedback may ensure a practically useful guaranteed stability region.

5. Conclusions

In this work, I presented an optimization-based computational method for determining Lyapunov functions and invariant regions for nonlinear dynamical systems. The starting point of the method is the approach presented in [1]. The improvements and new contributions can be summarized as follows:

1. The model transformation to the required form for optimization is done automatically using LFT and further algebraic model transformation steps. This technique results in the dimension reduction of the problem compared to known solutions in the literature.
2. An algorithm was given for the generation of appropriate annihilators for the vector π_b .
3. An improved method was proposed for determining the largest possible invariant set for the dynamics using the computed Lyapunov function.
4. A simplified formula was given for the LMI, which ensures the negative definiteness of the Lyapunov function. The simplification was done by merging the two annihilators of π_b from the representation (2.11). The formula does not require the system matrix $F(x)$ to be quadratic in the model (2.11). Therefore, it can be considered as a generalization of the formula presented in [1].

The operation of the approach was illustrated through examples taken from the literature. The results confirmed the applicability of the proposed method, and the estimated DOAs were very similar or bigger than in [1]. It is worth mentioning again the third order rational system in Section 4.4, for which I obtained approximately 10 times larger DOA than the authors in [1].

Although the method is appropriate only for rational systems, it was adopted on the model of the inverted pendulum with state feedback, that contains trigonometric terms as well. These terms were approximated by 2nd order Taylor polynomials, finally obtaining a rational system.

The method was applied for the stability analysis of a simple continuous bioreactor model. The Lyapunov functions for the open and closed loop cases, were successfully computed and the corresponding guaranteed stability regions were determined for different feedback gains.

Future plans, possible improvements

In the future, we aim to automate the iterative evaluation of the polytope \mathcal{X} in which the Lyapunov conditions are required to be satisfied. Furthermore, we aim to test the algorithm on even higher dimensional system models assuming rectangular polytope \mathcal{X} , and it is also motivating to analyse the performance of different dynamical or nonlinear control feedback laws. Finally, our plan is to study the evaluation of the possible annihilators based on the conservativeness of the corresponding LMI conditions, while the number of decision variables of the optimization problem is kept as low as possible.

Acknowledgement

I would like to express my appreciation to my supervisor, Dr. Gábor Szederkényi, who coordinated and helped my work tirelessly. Furthermore, I say many thanks to Dr. Péni Tamás, whose suggestions proved to be essential during my work. I would like to convey my gratitude to Bernadett Ács, who helped me in writing this report. Finally, I gratefully acknowledge the support of grants OTKA NF104706, and KAP-1.1-15.

Bibliography

- [1] A. Trofino and T. J. M. Dezuo. LMI stability conditions for uncertain rational nonlinear systems. *International Journal of Robust and Nonlinear Control*, 2013.
- [2] G. Szederkényi, N. R. Kristensen, K. M. Hangos, and S. B. Jorgensen. Nonlinear analysis and control of a continuous fermentation process. *Computers and Chemical Engineering*, 26:659–670, 2002.
- [3] S. Boyd, L. El Ghaoui, E. Feron, and V. Balakrishnan. *Linear Matrix Inequalities in System and Control Theory*, volume 15 of *Studies in Applied Mathematics*. SIAM, Philadelphia, PA, June 1994.
- [4] Carsten W Scherer and Siep Weiland. Linear matrix inequalities in control. *Lecture Notes, Dutch Institute for Systems and Control, Delft, The Netherlands*, 2000.
- [5] J-F. Magni. Linear fractional representation toolbox (version 2.0) for use with matlab. *Free Web publication <http://www.cert.fr/dcsd/idco/perso/Magni>*, 2006.
- [6] S. Hecker, András Varga, and J-F. Magni. Enhanced LFR-toolbox for MATLAB. pages 25–29, 2004.
- [7] MOSEK ApS. *The MOSEK optimization toolbox for MATLAB manual. Version 7.1 (Revision 28).*, 2015.
- [8] J. Löfberg. Yalmip : A toolbox for modeling and optimization in MATLAB. In *Proceedings of the CACSD Conference*, Taipei, Taiwan, 2004.
- [9] Péter Polcz, Gábor Szederkényi, and Tamás Péni. An improved method for estimating the domain of attraction of nonlinear systems containing rational functions. In *Journal of Physics: Conference Series*, volume 659, page 012038. IOP Publishing, 2015.
- [10] Péter Polcz, Gábor Szederkényi, and Tamás Péni. An improved method for estimating the domain of attraction of uncertain rational nonlinear systems by using LMI stability conditions. *Jedlik Laboratories Reports*, volume III. no. 4., JLR-4/2015, pages 7–33, Pázmány University Press, Budapest, 2015.

- [11] Graziano Chesi. *Domain of attraction: analysis and control via SOS programming*, volume 415. Springer Science & Business Media, 2011.
- [12] Vladimir Ivanovich Zubov and Leo F Boron. *Methods of AM Lyapunov and their Application*. Noordhoff Groningen, 1964.
- [13] Fabio Camilli, Lars Grüne, and Fabian Wirth. A generalization of zubov’s method to perturbed systems. *SIAM Journal on Control and Optimization*, 40(2):496–515, 2001.
- [14] A. Vannelli and M. Vidyasagar. Maximal Lyapunov functions and domains of attraction for autonomous nonlinear systems. *Automatica*, 21:69–80, 1985.
- [15] Y. Ohta, H. Imanishi, L. Gong, and H. Haneda. Computer generated Lyapunov functions for a class of nonlinear systems. *IEEE Transactions on Circuits and Systems*, 40:343–354, 1993.
- [16] P. Giesl and S. Hafstein. Construction of Lyapunov functions for nonlinear planar systems by linear programming. *Journal of Mathematical Analysis and Applications*, 388:463–479, 2012.
- [17] Sz. Rozgonyi, K. M. Hangos, and G. Szederkényi. Determining the domain of attraction of hybrid non-linear systems using maximal Lyapunov functions. *Kybernetika*, 46:19–37, 2010.
- [18] Laurent El Ghaoui and Gérard Scorletti. Control of rational systems using linear-fractional representations and linear matrix inequalities. *Automatica*, 32(9):1273 – 1284, 1996.
- [19] U. Topcu, A. K. Packard, and P. Seiler. Local stability analysis using simulations and sum-of-squares programming. *Automatica*, 44(10):2669–2675, 2008.
- [20] U. Topcu, A. Packard, P. Seiler, and G. Balas. Robust region-of-attraction estimation. *IEEE Transactions on Automatic Control*, 55(1):137–142, 2010.
- [21] Carsten W W Scherer. A full block s-procedure with applications. In *Decision and Control, 1997., Proceedings of the 36th IEEE Conference on*, volume 3, pages 2602–2607. IEEE, 1997.
- [22] Jeremy G VanAntwerp and Richard D Braatz. A tutorial on linear and bilinear matrix inequalities. *Journal of Process Control*, 10(4):363–385, 2000.
- [23] Luiz FS Buzachero, Edvaldo Assuncao, Emerson RP Da Silva, and Marcelo CM Teixeira. *New techniques for optimizing the norm of robust controllers of polytopic uncertain linear systems*. INTECH Open Access Publisher, 2012.

- [24] MC de Oliveira, RE Skelton, and SO Reza Moheimani. Perspectives in robust control. *Perspectives in Robust Control*, 268, 2001.
- [25] Kemin Zhou, John Comstock Doyle, Keith Glover, et al. *Robust and optimal control*, volume 40. Prentice hall New Jersey, 1996.
- [26] V. Chellaboina, S. Bhat, M.M. Haddad, and D.S. Bernstein. Modeling and analysis of mass-action kinetics. *Control Systems, IEEE*, 29(4):60–78, Aug 2009.
- [27] E. E. Sel'kov. Self-oscillations in glycolysis. *European Journal of Biochemistry*, 3(1):79–86, 1968.
- [28] Thomas Wilhelm. The smallest chemical reaction system with bistability. *BMC Systems Biology*, 3(1), 2009.
- [29] D. Dochain, M. Perrier, and M. Guay. Extremum seeking control and its application to process and reaction systems: A survey. *Mathematics and Computers in Simulation*, 82:369–380, 2011.